Hydrol. Earth Syst. Sci. Discuss., 11, 12443–12488, 2014
www.hydrol-earth-syst-sci-discuss.net/11/12443/2014/
doi:10.5194/hessd-11-12443-2014
© Author(s) 2014. CC Attribution 3.0 License.

Hydrology and Earth System Sciences
Discussions
Open Access

This discussion paper is/has been under review for the journal Hydrology and Earth System Sciences (HESS). Please refer to the corresponding final paper in HESS if available.

Sampling frequency trade-offs in the assessment of mean transit times of tropical montane catchment waters under semi-steady-state conditions

E. Timbe[1,2], D. Windhorst[2], R. Celleri[3], L. Timbe[4], P. Crespo[1], H.-G. Frede[2], J. Feyen[1], and L. Breuer[2]

[1]Departamento de Recursos Hídricos y Ciencias Ambientales, Universidad de Cuenca, Cuenca, Ecuador
[2]Institute for Landscape Ecology and Resources Management (ILR), Research Centre for Bio Systems, Land Use and Nutrition (IFZ), Justus-Liebig-Universität Gießen, Gießen, Germany
[3]Facultad de Ciencias Agropecuarias, Universidad de Cuenca, Cuenca, Ecuador
[4]Facultad de Ciencias Químicas, Universidad de Cuenca, Cuenca, Ecuador

Received: 17 October 2014 – Accepted: 20 October 2014 – Published: 7 November 2014

Correspondence to: E. Timbe (edison_timbe@yahoo.com)

Published by Copernicus Publications on behalf of the European Geosciences Union.

Abstract

Stream and soil waters were collected on a weekly basis in a tropical montane cloud forest catchment for two years and analyzed for stable water isotopes in order to infer transit time distribution functions and to define the mean transit times. Depending on the water type (stream or soil water), lumped distribution functions such as Exponential-Piston flow, Linear-Piston flow and Gamma models using temporal isotopic variations of precipitation event samples as input, were fitted. Samples were aggregated to daily, weekly, biweekly, monthly and bimonthly time scales in order to check the sensitivity of temporal sampling on model predictions. The study reveals that the effect of decreasing sampling frequency depends on the water type. For soil waters with transit times in the order of weeks to months, there was a clear trend of over prediction. In contrast, the trend of prediction for stream waters, with a dampened isotopic signal and mean transit times in the order of 2 to 4 years, was less clear and depending on the type of model used. The trade-off to coarse data resolutions could potentially lead to misleading conclusions on how water actually moves through the catchment, while at the same time predictions can reach better fitting efficiencies, lesser uncertainties, errors and biases. For both water types an optimal sampling frequency seems to be one or at most two weeks. The results of our analyses provide information for the planning (in particular in terms of cost-benefit and time requirements) of future fieldwork in similar Andean or other catchments.

1 Introduction

The application of tracers and particularly environmental isotopes have become valuable and attractive tools in catchment hydrology, providing new insights in the allocation of water provenance (e.g. Barthold et al., 2010), runoff component identification and quantification (e.g. Ladouche et al., 2001), age dating and transit time distribution (TTD) of water (e.g. Timbe et al., 2014; Leibundgut et al., 2009; Kendall and McDonnell,

CC BY

1998). An important benchmark in the use of tracers in hydrology was provided by the contributions of Maloszewski and Zuber (1982, 1993), who described and applied the methodology of tracer dating in detail. In their approach, routing of water in a catchment was mathematically expressed by a lumped parameter TTD function, commonly solved by the convolution method. In this method, fundamental conditions are the homogeneity of the system and steady state conditions. Although presently more complex models considering time-variant conditions are being tested (e.g. Rinaldo et al., 2011; Botter et al., 2010, 2011) lumped model approaches are still widely used. It provides basic inferences of the water paths and the transit time of water (e.g. Muñoz-Villers and McDonnell, 2012; Hrachowitz et al., 2009a; Kabeya et al., 2006; Maloszewski et al., 2006; McGuire and McDonnell, 2006; Rodgers et al., 2005; McGuire et al., 2002; Soulsby et al., 2000; Dewalle et al., 1997; Timbe et al., 2014).

Ideally, the interpretation of environmental tracers by the means of lumped parameter models should be used along with hydrometric and chemical data as a complementary tool to support or contrast findings from those traditional methods (e.g. Crespo et al., 2012). However, in practice, many studies in this field based their main findings on environmental tracers alone. This is, in any case justifiable, either by their relative low cost and easy applicableness. Besides the classical chemical tracer (e.g. chloride) used in lumped parameter models, the use of environmental isotopes (i.e. stable water isotopes) has become an appealing alternative to infer the functioning processes of a hydrologic system (Leibundgut et al., 2009). Their use is often advisable as a first step to gain insights in the hydrology of a catchment, not only for poorly gauged catchments for which common constraints are: difficult access, harsh climate conditions or scarce funding. Insights of mean transit times (MTT) or TTD functions of streams, springs, groundwater or even soils waters to be gained by the application of lumped parameter models also can serve as a starting point towards employing an improved sampling campaign which integrates more sources of data, or other types of tracers (e.g. Kirchner et al., 2010; Stewart et al., 2010), not to mention a more accurate sampling length and frequency. Given this background, the widespread use of

CC BY

environmental tracers and lumped parameter models does not come as a surprise. The handling and processing of this type of data is becoming a routine process in hydrological research (e.g. McGuire and McDonnell, 2006). Along with the increase in application, uncertainty analyses of the inferred results are becoming a routine procedure.

Solutions, formerly based only on the best fit to a particular model, now frequently include a range of behavioral or possible solutions (Weiler et al., 2003; Vaché and McDonnell, 2006; McGuire et al., 2007; Hrachowitz et al., 2009a, 2010, 2013; Birkel et al., 2011; Capell et al., 2012; Muñoz-Villers and McDonnell, 2012; Timbe et al., 2014). However, an appropriate sensitivity analysis of the model parameters to factors such as the degree of temporal resolution of the input data used to calibrate the tracer based lumped models is still uncommon as it is in traditional rainfall–runoff modelling (McGuire and McDonnell, 2006).

Such an analysis is necessary; the predictions provided by steady-state approaches are simple approximations of the real functioning of a catchment system, although valid for groundwater systems or median conditions of waters. Predictions, however, could be very approximate since most steady-state analyses of published studies are based on relatively poor information in terms of temporal and spatial variability of environmental tracers due to sampling (Rinaldo et al., 2011). In this regard, using a conceptual-lumped model Birkel et al. (2010) found that high temporal resolution isotope data were beneficial, especially for model conceptualization and calibration. That assertion was corroborated by Hrachowitz et al. (2011) who found evidence of potential misleading insights for a small headwater catchment of Scotland, derived from a lumped model, when low sampling frequency data were used (e.g. monthly or bimonthly). Similarly, McDonnell et al. (2010) stated that high frequency data may enable to falsify the assumption of a time-invariant TTD. In theory, the temporal resolution of a data set depends on the field sampling frequency, which must be in accordance to the expected time scale of the transit or residence time of the analyzed waters (McGuire and McDonnell, 2006) (e.g. higher frequencies should be used for waters with short transit

HESSD
11, 12443–12488, 2014

times than for longer ones). However, in practice, this factor is often constrained by logistical reasons, especially in remote catchments.

Most of the available tracer studies looking for the TTD or MTT of a catchment are based on weekly, biweekly, and less common on monthly data. Rare are samplings at higher time scales than weekly (e.g. Kirchner et al., 2000; Birkel et al., 2010). Sometimes high temporal resolution measurements are used for the analysis of rainfall–runoff events at smaller spatial scales (e.g. hillslope), in which the transit time of fast flows of the order of hours to few days is being searched for. But for those cases, time-variant instead of steady state approaches are necessary (e.g. Heidbüchel et al., 2012; Rinaldo et al., 2011; Botter et al., 2011; Weiler et al., 2003; Barnes and Bonell, 1996). In general, the temporal resolution of the data employed to infer hydrological process understanding from lumped parameter models can influence the results, thereby making it difficult to compare predictions from different studies (Hrachowitz et al., 2011).

To gain insights from the effect of the sampling frequency on the results of lumped parameter models, we collected stable water isotope time series in a baseflow-dominated Ecuadorian tropical montane cloud forest catchment. Data were aggregated into diverse levels of temporal resolution in order to analyze the sensitivity of this resolution on the model parameters and results (e.g. MTT) and the respective TTD of three widely known lumped models. The time sequence of this study consists of around two years of high resolution samples of rainfall events, weekly grab samples of stream water in the outlet of the catchment of the Rio San Francisco and seven tributaries, and bulk water samples from six soils sites, collected in the lower part of the catchment at 0.25 m depth. In order to apply time-invariant approaches, for the analyzed waters, only baseflow or average conditions were considered.

The hypotheses on which this study is based are: (1) some temporal resolutions of input data could substantially influences the results of lumped parameter models (e.g. coarse temporal data resolution such as monthly or bimonthly can lead to misleading conclusions although the fitting efficiencies are high), even when baseflow or mean conditions are considered for the analyzed waters; in this regard (2) a sensibility

HESSD
11, 12443–12488, 2014

CC BY

analysis of the sampling resolution is essential as part of analyzing the suitability of a lumped-parameter model, similarities or divergences of results from diverse sampling trade-offs could provide insights on the degree of reliability of a particular sampling frequency.

2 Materials and methods

2.1 Study area

The study area of the Rio San Francisco catchment (76.9 km^2, Fig. 1) is located in the eastern escarpments of the Andean mountains in south Ecuador. The local tropical climate is mainly influenced by easterly trade winds and thus by the Atlantic circulation patterns (Beck et al., 2008a). According to the records of four meteorological stations established in 1998 within the study area the mean annual temperature ranges from 15 °C in the lower part of the study area (1957 m a.s.l.) to 10 °C on the ridges (3150 m a.s.l.), with an altitudinal gradient of −0.57 °C per 100 m. Annual precipitation ranges from 2500 to 4000 mm in wet years. A large rainfall gradient of 220 mm per 100 m exists (Bendix et al., 2008b). Fog precipitation contributes additional 5 to 35 % of measured tipping-bucket rainfall (Rollenbeck et al., 2011). Rainfall intensities are low, in general less than 10 mm h^{-1} and the relative humidity varies from 85 % in the lower parts to 96 % at the ridges.

The geology of the study area consists of sedimentary and metamorphic Paleozoic rocks of the Chiguinda unit with contacts to the Zamora batholith (Beck et al., 2008b). Major soil types are Histosols associated with Stagnasols, Cambisols and Regosols; Umbrisols and Leptosols are present to a lesser degree (Liess et al., 2009). The topography of the area has an altitudinal range of 1725 to 3150 m a.s.l. and is characterized by steep valleys with an average slope of 63 %. Landslides are present in the catchment, especially along the paved road between the cities of Loja and Zamora. Seven main tributaries feed the San Francisco River. Their catchment areas vary in size from

HESSD
11, 12443–12488, 2014

0.7 to 34.9 km^2 and in their land cover: the southern part of the catchment is covered by pristine primary forest and sub-páramo, while the northern part is covered by grassland, shrubland, secondary forest and sub-páramo. Presently 68 % of the catchment is covered by forest, 20 % by sub-páramo, 7 % is used as pastures and 3 % is degraded grassland covered with shrubs (Goettlicher et al., 2009; Plesca et al., 2012). The main river and its tributaries are perennial. The flashy reaction of the hydrograph are due to rainstorms (Fig. 2a), while the slowly varying underlying trend corresponds to groundwater contribution (baseflow), which accounts for 85 % of the total runoff (Table 1). Given the climate of the area, a continuous yearly growing season, the absence of snowmelt and the uniform precipitation distribution over the year, the hydrograph does not show marked seasonal differences. Main physical and hydrological features of the catchment and tributaries are presented in Table 1. Additional detailed information on the climate and ecosystem gradients of the research area can be found in Bendix et al. (2008a), Fiedler and Beck (2008) and Wilcke et al. (2008).

2.2 Hydrometric measurements

The main catchment outlet and its sub-catchments were equipped with water level sensors (mini-diver, Schlumberger Water Services, Delft, NL) to obtain continuous water level readings. Reference discharge measurements using the salt dilution method were made frequently during the time of sampling. However, due to the high variability of the river bed in the sites Pastos (QP), Zurita (QZ) and Ramon (QR), only records for the sub-catchments Francisco Head (FH), Navidades (QN), Milagro (QM) and Cruces (QC) and for the main outlet Planta (PL) were considered as reliable to calculate stage-discharge curves and hydrographs (see Fig. 2a for PL; abbreviations of names for all study sites are defined in Fig. 1 and Table 2). For the remaining sites, discharge measured at the moment of sampling was used. The hydrometric information was used to derive baseflow, applying the Water Engineering Time Series PROcessing tool (WETSPRO) (Willems, 2009), making it possible to discern between stream water samples

Discussion Paper | Discussion Paper | Discussion Paper | Discussion Paper |
HESSD
11, 12443–12488, 2014

CC BY

taken under baseflow and peak flow conditions. Since time invariant conditions are considered for the application of the chosen lumped parameter models, samples taken during peak flows were discarded.

2.3 Sampling scheme and isotopic analyses

From October 2010 until August 2012, weekly grab samples of stream water for isotopic analysis (δ^{18}O and δ^{2}H) were collected in 2 mL amber glass bottles in the catchment's outlet (Fig. 2b) and in seven of its tributaries (Fig. 1, Tables 1–2). These samples represent an instantaneous isotopic concentration in time. Soil water was sampled weekly from cumulative drainage water of six wick-samplers at 0.25 m below surface, located in two characteristic areas of the lower part of the research area (Fig. 1, Table 2). The first three devices were installed in September 2010 in forest land and the remaining three in November 2010 in pastures. The devices share a comparable altitudinal gradient between pastures and forest. Details of the wick-sampler construction are given by Timbe et al. (2014). Once per week (generally the same day for stream water sampling) the cumulated volume in each 2 L sampling bottle was registered and a 2 mL sample for isotopic analysis was taken. These samples represent the weekly average bulk isotopic composition of soil water. Sampling was, in a few occasions, disrupted by short dry periods (after one or two weeks without rainfall), for which, no water was found in the bottles.

For the same time span as for stream water, rainfall samples for isotopic analyses were taken after every rainfall event, in the lower part of the catchment at 1900 m a.s.l. Samples were collected manually in 1 L bottles using a Ø 25 cm funnel, placed at the top of 1.5 m standing pole. The end of every event of rainfall was marked by a time span of at least 30 min without rainfall. After each event, the corresponding sampling bottle was covered with a lid and stored for analysis within a week in 2 mL amber glass bottles. Only sample volumes > 2 mL were found suitable for permanent storage and measurements. Events with a sample volume < 2 mL were discarded. A total of 946

HESSD
11, 12443–12488, 2014

cc BY

samples during 515 rain days (average duration of 3.2 h, varying from 0.25 to 19 h, with maximum 11 events per day) (Fig. 2c).

Table 2 shows the total number of analyzed samples according to the type of water. The stable isotopes signatures of δ^{18}O and δ^{2}H are reported in this study in per mil value relative to the Vienna Standard Mean Ocean Water (VSMOW) (Craig, 1961). The water isotopic composition was analyzed by wavelength-scanned cavity ring down spectroscopy (WS-CRDS) with a precision of 0.1 ‰ for δ^{18}O and 0.5 for δ^{2}H (PicarroL1102-i, CA, US).

2.4 Isotopic gradient of rainfall

Given the large altitudinal gradient in the San Francisco basin, it is to be expected that the input isotopic signal of rainfall for every sub-catchment varies according to its elevation (Dansgaard, 1964). However, due to economic constraints, it is a common practice to infer the isotopic variation for a larger area based on only one sampling location. Samples are usually volume-weighted and bulked for a predefined time interval such as weeks or months (McGuire and McDonnell, 2006). For this research, the isotopic variation of rainfall through the catchment was inferred from the sampling point located at 1900 m a.s.l. by using the altitudinal isotopic gradient of −0.22 ‰ δ^{18}O, −1.12 ‰ δ^{2}H and 0.6 ‰ deuterium excess per 100 m elevation gain estimated by Windhorst et al. (2013) for the same investigated area. This altitude gradient was applied to the volume-weighted isotope signals under the assumption that the incoming rainfall signal is the sole source of water. Windhorst et al. (2013) evaluated the spatial and seasonal variation of stable isotopes of rainfall, concluding that only the altitude effect is significant and that in this factor there is no significant influence of temperature, relative humidity and precipitation amount or intensity. Since δ^{18}O or δ^{2}H where highly correlated, it is highly probable that similar estimations of MTT are derived either using δ^{18}O or δ^{2}H (Timbe et al., 2014). Therefore, in this study only δ^{18}O was selected for further analysis.

HESSD

11, 12443–12488, 2014

Sampling frequency trade-offs in the assessment of mean transit times

E. Timbe et al.

Title Page
Abstract | Introduction
Conclusions | References
Tables | Figures
◀| |▶
◀ ▶
Back | Close
Full Screen / Esc
Printer-friendly Version
Interactive Discussion

cc BY

2.5 Lumped parameter equation to infer mean transit times of water

For the calculation of the MTT, the lumped parameter approach was utilized. The lumped approach considers the aquifer system as an integral unit, while the flow pattern is assumed to be constant. The transport of a tracer through a catchment can be deducted from the following general equation:

$$C_{\mathrm{out}}(t) = \int_{-\infty}^{t} C_{\mathrm{in}}(t')\exp[-\lambda(t-t')]g(t-t')\mathrm{d}t'. \tag{1}$$

In Eq. (1), known as the convolution integral equation, the tracer's outflow composition C_{out} at a time t (time of exit) consists of the tracer's input composition C_{in} that falls uniformly on the catchment in a previous time step t' (time of entry). C_{out} is lagged according to a TTD $g(t-t')$. The factor $\exp[-\lambda(t-t')]$ is used to correct for decay when a radioactive tracer is used (λ = tracer's radioactive decay constant). For stable tracers ($\lambda = 0$), considering a time span $t-t'$ and a tracer transit time τ, Eq. (1) can be rewritten as Eq. (2):

$$C_{\mathrm{out}}(t) = \int_{0}^{\infty} C_{\mathrm{in}}(t-\tau)g(\tau)\mathrm{d}\tau \tag{2}$$

where the transit time distribution TTD, known as the weighting function, is described by the normalized distribution function of the tracer $g(\tau)$ injected instantaneously over an entire area.

HESSD

11, 12443–12488, 2014

2.5.1 Transit time distributions of water

Widely known lumped parameter models applied to describe catchment's TTD function estimations were commented and applied in detail by Maloszewski and Zuber (1982) and since then were used in many other related studies (e.g. McGuire and McDonnell, 2006; Amin and Campana, 1996). Every model is based on considerations of the flow type which depends on the aquifer system. For instance, when using the Piston Flow Model (PFM) it is assumed that there are no flow lines with different transit times, and, hydrodynamic dispersion and molecular diffusion are negligible. In contrast, the Exponential Model (EM) considers that an exponential distribution of transit times exists, and that the mixing takes place only at the sampling site. The Linear Model (LM) assumes that distribution of transit times are constant: flow lines have equal velocity but linearly increasing flow times. The mentioned models are defined by only one parameter: the MTT of the tracer τ. In general it is unrealistic to expect that these simple models match the behavior of real systems. Therefore, two-parameter models consisting of the combination of two simple models such as the Exponential-Piston (EPM) or the Linear-Piston (LPM) are commonly used. The additional parameter η explains the portion of contribution of each type of flow. Two-parameter functions are more flexible than simpler models since they can represent various mixing possibilities (McGuire and McDonnell, 2006). Since the studies published by Kirchner et al. (2000, 2001), another widely known two-parameter function in tracer hydrology is the Gamma distribution model (GM) with the parameters shape α and scale β.

The optimal selection of a TTD is not that easy to achieve by direct or experimental methods (McGuire and McDonnell, 2006). A common practice is to assume a flow type system and to estimate the model parameters through a trial-and-error simulation-based process until "the best fit" to the observed data is obtained. According to previous insights for the same research area (Timbe et al., 2014), distribution functions such as GM (Eq. 3) and EPM (Eq. 4) yielded the best results when predicting the behavior of isotopic variation of the baseflow. GM and LPM (Eq. 5) provided the best matches to

CC BY

observed isotopic soil water data. The plausibility of these functions were shown by Timbe et al. (2014) in a detailed comparison of seven lumped models, including the EM, LM, GM, EPM, LPM, a Dispersion Model and the Two Parallel Linear Reservoir Model (Weiler et al., 2003). Hence, the following study explicitly investigates the model performance of the three pre-selected, most appropriate models:

$$g(\tau)_{\mathrm{GM}} = \frac{\tau^{\alpha-1}}{\beta^{\alpha}\Gamma(\alpha)} \exp\left(-\frac{\tau}{\beta}\right) \text{ for } \alpha > 0 \text{ and } \beta = \frac{\alpha}{\tau}, \tag{3}$$

$$g(\tau)_{\mathrm{EPM}} = \frac{\eta}{\tau} \exp\left(-\frac{\eta}{\tau} + \eta - 1\right) \text{ for } t \geq \tau(1-\eta^{-1}) \text{ or } 0 \text{ for } t < \tau(1-\eta^{-1}), \tag{4}$$

$$g(\tau)_{\mathrm{LPM}} = \frac{\eta}{2\tau}, \text{ for: } -\frac{\tau}{\eta} \leq t \leq \tau + \frac{\tau}{\eta} \text{ or } 0 \text{ for other } \tau. \tag{5}$$

2.5.2 Model performance

For the calibration of every lumped parameter model and type of water, we used the convolution method between the tracer's input signal (i.e. isotopic rainfall time series) and the expected TTD. The results were then compared with the observed variation in the respective analyzed effluent (e.g. stream or soil water).

For every simulation the goodness of fit, as defined by the Nash–Sutcliffe Efficiency coefficient NSE (Nash and Sutcliffe, 1970), was calculated comparing predictions to observed data. To automate and standardize the equation's resolution, we repeated 10 000 simulations by randomly sampling using the Monte Carlo based Generalized Likelihood Uncertainty Analysis (GLUE) (Beven and Freer, 2001) method. Behavioral solutions were selected for every case based on a lower limit dependent on the best NSE reached for every case. In our case, the lower limit was establish at 5 %, and the weighted quantiles between 0.05 and 0.95 (90 % of the behavioral limits) were calculated. From these values, in order to ease inter-comparisons, for every simulation the magnitude of uncertainty for each predicted parameter was calculated by subtracting the lower behavioral limit from the maximum one ($\Delta\tau, \Delta\alpha, \Delta\eta$). For the best predictions, the Root Mean Square Error (RMSE) and the BIAS were calculated to account

HESSD
11, 12443–12488, 2014

cc BY

for errors and deviations of predictions. In both cases they were reported in per mil (‰) units.

In most simulations, the convergence of solutions towards one solution peak was clearly defined within a predefined fixed range dependent on the type of model: τ [0–10 yr], α [0.01–10], η [1–10]. In cases with more than one solution peak, the largest peak was selected for the second model parameter in order to improve the convergence of the parameter that identifies the MTT of the tracer τ.

To get more stable results an artificial warm up period of 40 years was generated by repeating measured two year isotopic rainfall time series 20 times in a loop. This is a common practice when the seasonality of the inter-annual signal is repetitive and well defined (Hrachowitz et al., 2011; Muñoz-Villers and McDonnell, 2012).

2.6 Temporal resolution of data

As explained earlier, solving the convolution method requires a fixed time step for the input function C_{in}, which in turn will be the same time step resolution of the predicted output data C_{out}. In order to check the effect of the time resolution of the input data on the predictions, the simulations were performed by aggregating high resolution samples of rainfall (i.e. per event) into five levels of temporal resolution: daily, weekly, biweekly, monthly and bimonthly. For each data set, the isotopic composition for every event was weighted according to the collected volume for the considered time span, thereby yielding bulk isotopic signals as if they had been collected over the entire corresponding sampling interval (Fig. 3). For time spans corresponding to zero rainfall, the isotope signal of the antecedent time step was used. By using a predefined TTD function $g(\tau)$, Eq. (1) could be solved and it became possible to derive the best possible fit to the observed data for every outflow by varying the model parameters. Depending on how we aggregated the data, two distinct scenarios were considered.

Scenario 1: for every sampled site, observed isotopic data series of rainfall and outflows, stream and soil waters, were aggregated into coarser levels of data resolution. Since the finest resolution of outflow waters was weekly, we used this data resolution to

CC BY

calibrate models having daily rainfall data sets as input. For weekly, biweekly, monthly and bimonthly data sets, we used the corresponding time step resolution. For stream water, due to the smooth variation between two successive isotopic data, no volumetric weighting was applied, but a simple averaging of weekly isotopic values (e.g. a monthly value results from an averaging of four weekly values). For soil water, volumetric weighting was applied.

Scenario 2: diminishing the sampling resolution in both types of observed data at the same time (rainfall and outflows), as performed in Scenarios 1, could lead to incomplete insights, if we consider that coarse data resolutions, such as monthly or bimonthly, could provide lesser uncertainties or better simulation statistics than finer data resolutions (by the simple fact that less data is involved in the analyses). In this regard, a second scenario was set up, in which only the highest temporal resolution data of observed outflows (i.e. weekly) was considered for calibration, while the rainfall data used as input functions for the diverse temporal resolutions were considered the same as in Scenario 1. Results from this second scenario, facilitates to discern the adequacy of a particular time resolution over another.

It should be noted that, given these considerations, the predictive results for daily and weekly time resolutions are the same for both scenarios. For data resolutions larger than weekly, the combination of two different levels of information in the same lumped predictive model (e.g. monthly data for the input function of rainfall and weekly for the observed outflows) was handled through considering weekly time steps, although originally those rainfall values were derived as volumetrically weighted rainfall data from biweekly, monthly or bimonthly sampling resolutions.

Analysis of these two scenarios provides a quantifiable effect of data resolution on parameter estimation of the applied models. For comparative purpose among sampling trade-offs, for our study, the finest temporal resolution (i.e. daily rainfall and weekly outflow data) was considered as the main reference in order to define a particular result as lower or higher estimate. In order to look for similarities, divergences and trends between predictions, results were visually compared using Box–Whisker plots and the respective median (expressed in this text with a tilde on the top of a parameter symbol, e.g. $\widetilde{\tau}$) for the grouped six soil water sites and the eight stream water sites. Interpretation of the physical meaning of results considers that the MTT of water can be adequately characterized by the MTT of the tracer (τ).

3 Results

3.1 Soil water

3.1.1 Type 1 scenarios (Table 3, Fig. 4)

Using the GM or LPM the best predictions of the mean transit time (τ) as defined by the NSE, showed a clear increasing trend of this parameter vs. a decreasing temporal sampling resolution. For GM the median τ value ($\widetilde{\tau}$) for the finest sampling resolution (i.e. daily rainfall data, from here on also referred as the reference sampling resolution) was 4.7 weeks, while for weekly and biweekly resolutions data this value slightly rose to 5.2 and 5.9 weeks, an increase respectively of 10.5 and 26.4 %. Considering coarser data resolutions, as monthly or bimonthly, the obtained mean transit time even went up to 6.6 and 9.0 weeks, corresponding to a 42.1 and 92.9 % increase. The values and the corresponding trend for LPM were similar to the one obtained using GM. For LPM $\widetilde{\tau}$ varied from 4.6 to 8.9 weeks using the finest and the coarsest time resolutions, respectively. In general, GLUE based uncertainties for τ estimations, as defined by median values, ($\widetilde{\Delta\tau}$) were lower using daily rather than coarser sampling resolutions. In this regard, larger differences were found for LPM ranging from 1.4 weeks using daily data to 3.5 weeks using bimonthly data; while for GM the range of uncertainty varied from 1.8 to 2.1 weeks.

Estimations for GM's α parameter, showed a similar median value for daily, weekly or biweekly time resolutions ($\widetilde{\alpha}$ varied from 1.88 to 1.95), while the parameter was overestimated for coarser time resolutions; as for example the value was 3.73 for monthly

HESSD
11, 12443–12488, 2014

CC BY

and 4.51 for bimonthly data. On the other hand, using LPM, the variation of the median value of η only slightly changed among time resolutions (e.g. $\tilde{\eta}$ varied from 1.02 for daily up to 1.14 for bimonthly data). However, for coarser data, such as monthly or bimonthly, results for particular sites showed larger values (e.g. for the A soil site η varied from 1.02 for daily data to 1.40 for bimonthly data). Median values of GLUE-based uncertainties for these parameters did not show a clear trend or significant variation as a function of the time resolution. In all cases $\widetilde{\Delta\alpha}$ varied between 2.13 and 3.09 weeks, while $\widetilde{\Delta\eta}$ varied from 0.17 to 0.45 weeks.

Median values of NSE for GM and LPM were rather similar; ranging between 0.76 to 0.86. Likewise, for both models the RMSE and BIAS were comparable between time resolutions.

As a typical case among soil water sites Fig. 5 depicts results of the convergence of model parameters, simulated vs. observed $\delta^{18}O$ seasonality, and predicted residence time distribution function, using the GM for every temporal data resolution.

3.1.2 Type 2 scenarios (Table 4, Fig. 4)

Compared to type 1 scenarios parameter results and uncertainties among time resolutions were more stable. Using GM $\tilde{\tau}$ for the finest and coarsest time resolutions varied between 4.7 and 5.0 weeks, and $\widetilde{\Delta\tau}$ extreme values between 1.8 and 2.1 weeks, respectively. The variation of α between sampling frequencies was also smaller: $\tilde{\alpha}$ was between 1.73 and 2.23, while $\widetilde{\Delta\alpha}$ was similar to results from type 1 scenarios (e.g. smaller uncertainties for finer than coarser resolution data sets: 2.99 for daily data sets and 4.25 for bimonthly data). However there were larger uncertainties for particular sites when coarse resolution data sets were used (e.g. the most extreme case was accounted for the A site where there was a $\Delta\alpha$ increase from 2.83 using daily data to 18.82 using bimonthly data). Using LPM the trends and values were similar to the ones obtained with GM. Comparing the daily and bimonthly time resolutions $\tilde{\tau}$ varied from 4.6 to 5.3 weeks, and their respective $\widetilde{\Delta\tau}$ ranged from 1.4 to 1.7 weeks. The median value for η was around 1 for all sampling frequencies. Although small for all cases, $\widetilde{\Delta\eta}$

CC BY

was larger for coarser than for finer time resolution data: 0.36 for daily up to 0.56 for bimonthly data.

For both models, the NSE, RMSE and BIAS of the best predictions followed similar trends as for type 1 scenarios. When compared to results from the reference sampling resolution, NSE values were higher for weekly and biweekly input data. For instance, using GM, the median value of the best NSEs was 0.81 for daily and 0.84 for both weekly and biweekly data. Monthly data sets provided predictions with similar efficiencies, while for bimonthly data the median value of NSE was 0.78, the lowest among all sampling resolutions of type 2 scenarios.

3.2 Stream water

3.2.1 Type 1 scenarios (Table 5, Fig. 6)

Using GM, parameter results revealed lower values of τ for coarser time resolutions data when compared to daily data resolution, e.g. $\tilde{\tau}$ went from 2.1 yr for daily data to 1.2 yr for bimonthly data. Furthermore, a clear decreasing trend of uncertainty lengths was detected. In general $\Delta\tau$ was smaller for coarser than for finer time resolution data: $\widetilde{\Delta\tau}$ was 1.7 yr for daily data while 0.6 yr for bimonthly data. The GM's α showed a trend to higher values proportional to the decrease of sampling resolution: $\tilde{\alpha}$ was 0.63 for the reference while it reached a value of 0.93 for bimonthly data. The median values of uncertainty lengths for this parameter $\widetilde{\Delta\alpha}$ only slightly increased from daily (0.14) to the coarsest data resolution (0.18). On the other hand, for the same conditions using EPM, τ values only slightly increase with coarser time resolutions ($\tilde{\tau}$ varied from 2.7 to 3.0 yr between daily and bimonthly data resolutions), whereas $\Delta\tau$ vary little with sampling frequency. Extreme $\widetilde{\Delta\tau}$ values were accounted for daily and bimonthly data: 0.28 and 0.37 yr, respectively. The parameter η, as a median value among sites, depicted subtle smaller values for coarser sampling frequencies. It decreased from 3.01 for daily data to 2.60 for bimonthly ones. In general, $\Delta\eta$ slightly decreased for coarser time resolutions: $\widetilde{\Delta\eta}$ dropped from 0.59 using daily to 0.46 using bimonthly data.

HESSD
11, 12443–12488, 2014

cc BY

Mostly and for both models the best solutions, as described by their NSEs, showed an increasing trend from finer to coarser data resolutions. For GM, median NSE values of 0.74 and 0.79 were reached using monthly and bimonthly data while for daily data it was 0.60. Analogously RMSE values were smaller for coarse data resolutions, median RMSE declined from 0.31 ‰ for daily to 0.17 ‰ for bimonthly data. BIAS remained small for all cases, with an average value of 0.04 %. For EPM we obtained similar trends and values.

Results for particular sites, follow nearly the trends described by the median values for all analyzed sites. Similarly, to the results depicted in Fig. 5 for the soil site C2, Fig. 7 depicts the variation in results for different data resolutions applied to the stream water of the main outlet of the catchment (PL).

3.2.2 Type 2 scenarios (Table 6, Fig. 6)

Similar to soil waters, and for both models, the variation of parameter results among diverse temporal resolution data was smaller than for the corresponding type 1 scenarios. When GM was used, $\widetilde{\tau}$ predictions varied from 2.1 yr for daily data to 1.8 yr for bimonthly. The largest estimated $\widetilde{\alpha}$ was 0.71 (using bimonthly data) close to 0.63, a value predicted using daily data. Uncertainty lengths for both parameters for the diverse temporal resolution data yielded similar average estimations: $\widetilde{\Delta\tau} \approx 1.6$ yr and $\widetilde{\Delta\alpha} \approx 0.14$. Also for the EPM model did the best solution parameters slightly vary amongst data resolutions. For example, considering daily and bimonthly data resolutions $\widetilde{\tau}$ predictions varied from 2.71 to 2.81 yr and $\widetilde{\eta}$ from 3.01 to 2.81. Uncertainties for both parameters were small and similar between time resolutions: $\widetilde{\Delta\tau}$ ranged from 0.28 to 0.30 yr and $\widetilde{\Delta\eta}$ from 0.59 to 0.51.

Contrary to type 1 scenarios, the median NSE decreased for coarser temporal resolution data; e.g. NSE for GM dropped from 0.60 using daily data to 0.44 using bimonthly ones. The value of RMSE and BIAS remained low amidst the temporal resolutions. Median RMSE was around 0.33 ‰ while the BIAS was 0.05 ‰. The trend of NSE values for EPM was similar to GM, although less sensitive to temporal resolution data. It declined

cc BY

from a median of 0.60 for daily data to 0.54 for bimonthly. RMSE and BIAS yielded for GM and EPM were comparable.

4 Discussion

4.1 Sensitivity of model-parameter results to sampling frequency

For soil and stream waters, we found significant differences between parameter results derived from higher and coarser data resolutions. Model parameters τ, α and η for type 1 scenarios (Tables 3 and 5, Figs. 4–7) showed distinct values between results obtained from finer resolution data, such as daily, weekly or biweekly, and coarser data resolutions, such as monthly or bimonthly. Keeping this finding in mind, a sensitivity analysis considering the effect of sampling frequency should be a common part of the workflow while applying lumped parameter models to estimate the TTD and MTT. Nevertheless only two studies could be found in recent literature, which deal with this sampling effect issue: Hrachowitz et al. (2010) using the gamma distribution model and Birkel et al. (2010) through adding information from tracers to a lumped-conceptual hydrological model.

For soil waters, with characteristic mean transit times of the order of a few weeks to months, an increasing trend of τ predictions related to a decrease of sampling data frequency was clear for GM and LPM. Using GM, model α predictions were similar for time resolutions up to biweekly sampling ($\alpha \approx 1.9$), but they were significantly higher for coarser data resolutions: median values were 3.73 and 4.75 for monthly and bimonthly data, respectively.

Using the gamma distribution for stream water, with characteristic MTT in the order of 2 to 4 years, parameter predictions for the main catchment outlet and its seven sub-catchments provided a different trend than found for soil waters. Predictions for τ yielded lower values for decreasing input resolution data (e.g. median τ values for stream water sites decreased from 2.1 yr using the daily data to 1.2 yr using bimonthly

CC BY

data). The descending trend depicted for τ values matched the increasing trend of α predictions, for which the median ranged from 0.63 for daily to 0.93 for bimonthly resolutions. These results show a distinct tendency than the one obtained by Hrachowitz et al. (2011) using the same distribution function and convolution method, and using chloride as tracer. In their case, a decreasing sampling frequency (i.e. from weekly to bimonthly) went hand in hand with a decreasing trend of α: from 0.689 for weekly to 0.276 for bimonthly datasets. The latter in turn, affected τ estimates resulting in systematically larger values, from 216 to 881 days. The best prediction of τ for the headwater catchment analyzed by Hrachowitz et al. (2011) (in the referred study the results obtained with the highest resolution available – weekly –, were considered as the reference solution) indicated stream waters with short MTT, around 0.59 yr, and a characteristic α value around 0.5, while in our case the best predictions of τ for all stream waters were larger than 2 yr and α values varied around 0.6. Even though any further comparison of the two studies is difficult, as they represent two different hydrological systems and therefore favor different distribution functions and shape parameters to describe the transport processes at hand, it can be seen that the MTTs greatly differ in accordance with the chosen sampling frequency.

Considering the GLUE-based uncertainties derived from type 1 scenarios, results between soil and stream water were contrasting. For the soil waters, uncertainty magnitudes $\Delta\tau$ remained similar (or slightly larger) with decreasing time resolution, while for stream water they were systematically shorter. Additional insights on the degree of the mismatch of coarser data resolutions compared to finer ones, were provided when using type 2 scenarios (Tables 4 and 6, Figs. 4 and 5), where the same weekly temporal resolution of observed data at outflows was kept for all sampled waters. For these cases, the NSE, RMSE and BIAS of the predictions were in general poorer for coarser data resolutions, hinting towards a higher reliability of finer resolution data sets. Besides the fact that parameter results derived from finer resolution data sets were more similar between each other, they did not show marked trends of either over- or underestimations compared to using type 1 scenarios.

HESSD
11, 12443–12488, 2014

Sampling frequency trade-offs in the assessment of mean transit times

E. Timbe et al.

CC BY

For our analyses, given the subtle divergence of results when using daily, weekly or even bi-weekly sampling resolutions, we consider them as adequate for the estimation of MTT and TTD. It should be noted that this finding is valid for groundwater systems or for mean conditions of soil water. In this regard, the utility of the highest sampling resolution, as daily or even sub-daily, could be noticeable when temporal dynamics are to be considered. In this regard Birkel et al. (2010) provided insights when dealing with the sampling frequency as part of the evaluation of the performance of a lumped-conceptual flow-tracer model, he found that the use of daily isotope data from rainfall and stream water, when compared to weekly or bi-weekly, besides providing higher fitting efficiencies, was beneficial for the conceptualization and calibration of that model.

4.2 Comparison of distribution functions

According to NSE values, the gamma distribution function (GM) performed slightly better than the other models (Tables 3–6), i.e. LM for soil water and EPM for stream water. However, using the GLUE approach for stream water the GM distribution function provided larger uncertainties than EPM (Fig. 6), hindering the clear preference of one model over another. The magnitude of uncertainties (i.e. behavioral solutions) could be a normal consequence of the highly damped isotopic signal of analyzed outflows, a common characteristic of all our stream water samples.

For stream waters, regardless of the data resolution set used, EPM showed lesser sensitiveness than GM when accounting for model parameter variations, which derived in MTT predictions more similar between sampling sites (Tables 5 and 6, Fig. 6). We should take these predictions with care since this behavior could also be the result of using a simple model or inadequate data sets, that are not sufficiently sensitive to distinguish between various TTD (McGuire and McDonnell, 2006; McGuire et al., 2005; Kirchner et al., 2000).

As lumped-model parameters are averaged metrics, a comparison of distribution functions between the tested models is preferred. For soil waters LPM yielded similar τ predictions than GM. However, a simple look at both distribution functions

CC BY

demonstrates that the gamma distribution function can provide more detailed information on how and when the tracer's signal increases/decreases and when the peak occurs. This is in line with the non-linearity of most processes in watersheds (Phillips, 2003; McDonnell, 2003). Notwithstanding, linear functions such as LPM are often used as a first approximation, despite presenting a simplification of the water movement of real systems (Fig. 8).

Comparing predicted GM and EPM distribution functions in the case of stream water, shows that EPM traces a peak signal delayed over time. We estimated η values between 2.15 and 3.23, the largest values we found in related studies that used the same distribution function. Reported values are normally lower than 2 (e.g. Hrachowitz et al., 2009a; Katsuyama et al., 2009; McGuire and McDonnell, 2006; Viville et al., 2006; Kabeya et al., 2006), indicating that a large portion of "old" water is released first to the river as depicted by the isotopic composition of the stream. At the contrary, when analyzing the behavior of water flow derived from the gamma distribution, the tracer signal's peak at the outflow occurs instantaneously, meaning that a considerable portion of the event rainfall water rapidly contributes to discharge, as for instance via lateral flow from near-surface deposits. Over time, the tracer signal decreases (for either EPM or GM), but once again the implications are different for both models comparing their flow recessions. As shown in Fig. 8, the tracer signal decreases more rapidly for EPM than for GM. Thus, depending on which distribution function is used, the interpretation is different. For example, in water management using the EPM predictions one could argue that the effects of contamination of water sources will not be immediately reflected in the river water and further that its effect will be rather quickly disappearing. Contrary, inferences provided by a gamma distribution would tell that pollutants in the catchment would have an instantaneous impact on the river water and that the effect will sustain longer over time.

The adequacy of using a gamma distribution to represent a real system has been widely assumed and discussed (e.g. Kirchner et al., 2001, 2010; Schumer et al., 2003; Hrachowitz et al., 2009a, b, 2010, 2011; Soulsby et al., 2009, 2010; Dunn et al., 2010;

HESSD
11, 12443–12488, 2014

CC BY

Godsey et al., 2010; Speed et al., 2010; Maher, 2011; Birkel et al., 2012; Capell et al., 2012; Heidbüchel et al., 2012; McGrane et al., 2014) since the bench mark paper published by Kirchner et al. (2000) in which they used chloride based tracers and spectral methods with high frequency sampling. As stated by Kirchner et al. (2010), the gamma distribution accounts in a more complete way the spectral range of waters with larger and shorter distribution functions. This results in a more realistic description of the distribution of water, when compared to other two-parameter and linear distribution functions. Corroborating these findings, Stewart et al. (2010) discovered that when using tritium isotopes the flow recessions are significantly longer than they are predicted using δ^{18}O or δ^{2}H isotopes.

Considering a gamma distribution for our basin, the MTT varied between 2 and 4 years and α between 0.54 and 0.68, using finer sampling resolutions. This range of α values is similar to findings from other tracers studies on stream water using spectral analyses and high resolution samples of chloride. Kirchner et al. (2000) demonstrated, using the spectral analysis methods, that an α value of approximately 0.5 provides a more proper representation of several stream waters in Wales. As stated by Soulsby et al. (2010) gamma distributions with $\alpha < 1$ are most suitable to represent non-linear processes. Similarly several other studies found α values significantly smaller than 1 (McGuire et al., 2005; Hrachowitz et al., 2009a, 2010; Godsey et al., 2010; Kirchner et al., 2010; Speed et al., 2010; Birkel et al., 2012; Heidbüchel et al., 2012; Muñoz-Villers and McDonnell, 2012). On the other hand, our results reported that when coarser time resolutions were used (monthly or bimonthly) the value of α approached 1. Given an $\alpha = 1$, the GM model yields equivalent predictions as a pure exponential model, which could lead to erroneous deductions.

At shorter time scales, as for soil waters in comparison to the previously discussed stream water, the gamma distribution function was characterized by a delayed occurrence of the tracer's peak ($\alpha \approx 2$). For soil waters, although similar insights in terms of τ could have been inferred from other models, the linear distribution function of the TTD seems to oversimplifies the water flow processes in the catchment (Fig. 8).

HESSD
11, 12443–12488, 2014

Differences between trends for shorter (i.e. soil waters) and longer MTT (as for stream water) seem to be related to the shape of the MTT distribution function, when considering a gamma distribution for instance, for $\alpha \leq 1$ the tracer's peak signal occurs at the beginning while for $\alpha > 1$ it is delayed in time, which indicates different processes for each water type (Dunn et al., 2010). For our study catchment, considering that NSE are high for all models and that TTD does not seem to influence their performance but greatly influences the predicted MTT, additional insights need be explored in order to unveil the correct TTD-function as solely relying on model performances could lead to misleading results. In this regard, studies at smaller spatial scales using high sampling frequencies and time variant conditions should be performed in order to cover a wider spectral range of waters.

5 Conclusions

Environmental tracer data of rainfall, stream and soil water were collected in the San Francisco catchment with the objective to delineate the reliability of transit time predictions as a function of the input data resolution. The collected information was used to test the prediction accuracy of commonly used lumped models with respect to sampling frequency. Compared to results from coarse data sets, finer temporal resolutions provided more similar outputs. Overall, discrepancies between predictions of diverse sampling frequencies point out that the assessment of the convergence and sensitivity of model parameters is essential defining TTD through model calibration (McGuire and McDonnell, 2006).

The question arises which distribution function should be used that best depicts the processes of the analyzed waters. In this regard, for soil water the gamma distribution not only provides the highest goodness of fit but also more realistic and meaningful predictions; although for dampened isotopic signals (i.e. stream waters) a model preference is still not clear, besides model parameters seem to be more sensitive to sampling frequencies, increasing considerably the risk of misinterpretation of the underlying

CC BY

processes, for these cases more research is still needed in order to account the more reliable distribution function.

The study clearly demonstrates that estimations of the TTDs for micro-catchments in the same region using different frequencies of data sampling provides an additional source of uncertainty, which might hinder a correct model comparison and misrepresentation of the water routing system. The present research also provides a better framework for future sampling strategies in the San Francisco basin and similar basins in the Andean mountain region. Based on the new insights presented in this manuscript more elaborated sampling campaigns could be undertaken, which would contribute to a more efficient management of the water resources of Andean and similar mountain basins. In particular, the performance of steady state modeling approaches can be considerably improved increasing the sampling frequency, offering an indirect way to account for the time-variable conditions.

Acknowledgements. The authors our grateful to Karina Feijo for her valuable help during field work and to Irene Cardenas for the assistance provided during the multitude of lab analyses. Furthermore, we like to acknowledge the financial support of the German Research Foundation (DFG, BR2238/4-2) and the Secretaría Nacional de Educación Superior, Ciencia, Tecnología e Innovación (SENESCYT), without which this research could not have been realized.

References

Amin, I. E. and Campana, M. E.: A general lumped parameter model for the interpretation of tracer data and transit time calculation in hydrologic systems, J. Hydrol., 179, 1–21, doi:10.1016/0022-1694(95)02880-3, 1996.

Barnes, C. J. and Bonell, M.: Application of unit hydrograph techniques to solute transport in catchments, Hydrol. Process., 10, 793–802, doi:10.1002/(SICI)1099-1085(199606)10:6<793::AID-HYP372>3.3.CO;2-B, 1996.

Barthold, F. K., Wu, J., Vaché, K. B., Schneider, K., Frede, H.-G., and Breuer, L.: Identification of geographic runoff sources in a data sparse region: hydrological processes and the limitations of tracer-based approaches, Hydrol. Process., 24, 2313–2327, doi:10.1002/hyp.7678, 2010.

Discussion Paper | Discussion Paper | Discussion Paper | Discussion Paper |

CC BY

Beck, E., Kottke, I., Bendix, J., Makeschin, F., and Mosandl, R.: Gradients in a tropical mountain ecosystem – a synthesis, in: Gradients in a Tropical Mountain Ecosystem of Ecuador, vol. 198, edited by: Beck, E., Bendix, J., Kottke, I., Makeschin, F., and Mosandl, R., Springer, Berlin, 451–463, 2008a.

Beck, E., Makeschin, F., Haubrich, F., Richter, M., Bendix, J., and Valerezo, C.: The ecosystem (Reserva Biológica San Francisco), in: Gradients in a Tropical Mountain Ecosystem of Ecuador, edited by: Beck, E., Bendix, J., Kottke, I., Makeschin, F., and Mosandl, R., Springer, Berlin, 1–13, 2008b.

Bendix, J., Rollenbeck, R., Fabian, P., Emck, P., Richter, M., and Beck, E.: Climate variability, in: Gradients in a Tropical Mountain Ecosystem of Ecuador, edited by: Beck, E., Bendix, J., Kottke, I., Makeschin, F., and Mosandl, R., Springer, Berlin, 281–290, 2008a.

Bendix, J., Rollenbeck, R., Richter, M., Fabian, P., and Emck, P.: Climate, in: Gradients in a Tropical Mountain Ecosystem of Ecuador, edited by: Beck, E., Bendix, J., Kottke, I., Makeschin, F., and Mosandl, R., Springer, Berlin, 63–73, 2008b.

Beven, K. and Freer, J.: Equifinality, data assimilation, and uncertainty estimation in mechanistic modelling of complex environmental systems using the GLUE methodology, J. Hydrol., 249, 11–29, doi:10.1016/S0022-1694(01)00421-8, 2001.

Birkel, C., Dunn, S. M., Tetzlaff, D., and Soulsby, C.: Assessing the value of high-resolution isotope tracer data in the stepwise development of a lumped conceptual rainfall–runoff model, Hydrol. Process., 24, 2335–2348, doi:10.1002/hyp.7763, 2010.

Birkel, C., Tetzlaff, D., Dunn, S. M., and Soulsby, C.: Using lumped conceptual rainfall–runoff models to simulate daily isotope variability with fractionation in a nested mesoscale catchment, Adv. Water Resour., 34, 383–394, doi:10.1016/j.advwatres.2010.12.006, 2011.

Birkel, C., Soulsby, C., Tetzlaff, D., Dunn, S., and Spezia, L.: High-frequency storm event isotope sampling reveals time-variant transit time distributions and influence of diurnal cycles, Hydrol. Process., 26, 308–316, doi:10.1002/hyp.8210, 2012.

Botter, G., Bertuzzo, E., and Rinaldo, A.: Transport in the hydrologic response: travel time distributions, soil moisture dynamics, and the old water paradox, Water Resour. Res., 46, W03514, doi:10.1029/2009WR008371, 2010.

Botter, G., Bertuzzo, E., and Rinaldo, A.: Catchment residence and travel time distributions: the master equation, Geophys. Res. Lett., 38, L11403, doi:10.1029/2011GL047666, 2011.

HESSD

11, 12443–12488, 2014

Sampling frequency trade-offs in the assessment of mean transit times

E. Timbe et al.

CC BY

Capell, R., Tetzlaff, D., Hartley, A. J., and Soulsby, C.: Linking metrics of hydrological function and transit times to landscape controls in a heterogeneous mesoscale catchment, Hydrol. Process., 26, 405–420, doi:10.1002/hyp.8139, 2012.

Craig, H.: Standard for reporting concentrations of deuterium and oxygen-18 in natural waters, Science, 133, 1833, doi:10.1126/science.133.3467.1833, 1961.

Crespo, P., Bücker, A., Feyen, J., Vaché, K. B., Frede, H.-G., and Breuer, L.: Preliminary evaluation of the runoff processes in a remote montane cloud forest basin using mixing model analysis and mean transit time, Hydrol. Process., 26, 3896–3910, doi:10.1002/hyp.8382, 2012.

Dansgaard, W.: Stable isotopes in precipitation, Tellus, 16, 436–468, doi:10.1111/j.2153-3490.1964.tb00181.x, 1964.

Dewalle, D. R., Edwards, P. J., Swistock, B. R., Aravena, R., and Drimmie, R. J.: Seasonal isotope hydrology of three Appalachian forest catchments, Hydrol. Process., 11, 1895–1906, doi:10.1002/(SICI)1099-1085(199712)11:15<1895::AID-HYP538>3.3.CO;2-R, 1997.

Dunn, S. M., Birkel, C., Tetzlaff, D., and Soulsby, C.: Transit time distributions of a conceptual model: their characteristics and sensitivities, Hydrol. Process., 24, 1719–1729, doi:10.1002/hyp.7560, 2010.

Fiedler, K. and Beck, E.: Investigating gradients in ecosystem analysis, in: Gradients in a Tropical Mountain Ecosystem of Ecuador, edited by: Beck, E., Bendix, J., Kottke, I., Makeschin, F., and Mosandl, R., Springer, Berlin, 49–54, 2008.

Godsey, S. E., Aas, W., Clair, T. A., de Wit, H. A., Fernandez, I. J., Kahl, J. S., Malcolm, I. A., Neal, C., Neal, M., Nelson, S. J., Norton, S. A., Palucis, M. C., Skjelkvale, B. L., Soulsby, C., Tetzlaff, D., and Kirchner, J. W.: Generality of fractal $1/f$ scaling in catchment tracer time series, and its implications for catchment travel time distributions, Hydrol. Process., 24, 1660–1671, doi:10.1002/hyp.7677, 2010.

Goettlicher, D., Obregon, A., Homeier, J., Rollenbeck, R., Nauss, T., and Bendix, J.: Land-cover classification in the Andes of southern Ecuador using Landsat ETM plus data as a basis for SVAT modelling, Int. J. Remote Sens., 30, 1867–1886, doi:10.1080/01431160802541531, 2009.

Heidbüchel, I., Troch, P. A., Lyon, S. W., and Weiler, M.: The master transit time distribution of variable flow systems, Water Resour. Res., 48, W06520, doi:10.1029/2011WR011293, 2012.

CC BY

Hrachowitz, M., Soulsby, C., Tetzlaff, D., Dawson, J. J. C., Dunn, S. M., and Malcolm, I. A.: Using long-term data sets to understand transit times in contrasting headwater catchments, J. Hydrol., 367, 237–248, doi:10.1016/j.jhydrol.2009.01.001, 2009a.

Hrachowitz, M., Soulsby, C., Tetzlaff, D., Dawson, J. J. C., and Malcolm, I. A.: Regionalization of transit time estimates in montane catchments by integrating landscape controls, Water Resour. Res., 45, W05421, doi:10.1029/2008WR007496, 2009b.

Hrachowitz, M., Soulsby, C., Tetzlaff, D., Malcolm, I. A., and Schoups, G.: Gamma distribution models for transit time estimation in catchments: physical interpretation of parameters and implications for time-variant transit time assessment, Water Resour. Res., 46, W10536, doi:10.1029/2010WR009148, 2010.

Hrachowitz, M., Soulsby, C., Tetzlaff, D., and Malcolm, I. A.: Sensitivity of mean transit time estimates to model conditioning and data availability, Hydrol. Process., 25, 980–990, doi:10.1002/hyp.7922, 2011.

Hrachowitz, M., Savenije, H., Bogaard, T. A., Tetzlaff, D., and Soulsby, C.: What can flux tracking teach us about water age distribution patterns and their temporal dynamics?, Hydrol. Earth Syst. Sci., 17, 533–564, doi:10.5194/hess-17-533-2013, 2013.

Kabeya, N., Katsuyama, M., Kawasaki, M., Ohte, N., and Sugimoto, A.: Estimation of mean residence times of subsurface waters using seasonal variation in deuterium excess in a small headwater catchment in Japan, Hydrol. Process., 21, 308–322, doi:10.1002/hyp.6231, 2006.

Katsuyama, M., Kabeya, N., and Ohte, N.: Elucidation of the relationship between geographic and time sources of stream water using a tracer approach in a headwater catchment, Water Resour. Res., 45, W06414, doi:10.1029/2008WR007458, 2009.

Kendall, C. and McDonnell, J. J.: Isotope Tracers in Catchment Hydrology, Elsevier, Amsterdam, the Netherlands, 1998.

Kirchner, J. W., Feng, X. H., and Neal, C.: Fractal stream chemistry and its implications for contaminant transport in catchments, Nature, 403, 524–527, doi:10.1038/35000537, 2000.

Kirchner, J. W., Feng, X. H., and Neal, C.: Catchment-scale advection and dispersion as a mechanism for fractal scaling in stream tracer concentrations, J. Hydrol., 254, 82–101, doi:10.1016/S0022-1694(01)00487-5, 2001.

Kirchner, J. W., Tetzlaff, D., and Soulsby, C.: Comparing chloride and water isotopes as hydrological tracers in two Scottish catchments, Hydrol. Process., 24, 1631–1645, doi:10.1002/hyp.7676, 2010.

HESSD

11, 12443–12488, 2014

Sampling frequency trade-offs in the assessment of mean transit times

E. Timbe et al.

Ladouche, B., Probst, A., Viville, D., Idir, S., Baqué, D., Loubet, M., Probst, J.-L., and Bariac, T.: Hydrograph separation using isotopic, chemical and hydrological approaches (Strengbach catchment, France), J. Hydrol., 242, 255–274, doi:10.1016/S0022-1694(00)00391-7, 2001.

Leibundgut, C., Maloszewski, P., and Külls, C.: Environmental tracers, in: Tracers in Hydrology, John Wiley & Sons, Ltd., Chichester, UK, 13–56, doi:10.1002/9780470747148.ch3, 2009.

Liess, M., Glaser, B., and Huwe, B.: Digital soil mapping in southern Ecuador, Erdkunde, 63, 309–319, doi:10.3112/erdkunde.2009.04.02, 2009.

Maher, K.: The role of fluid residence time and topographic scales in determining chemical fluxes from landscapes, Earth Planet. Sc. Lett., 312, 48–58, doi:10.1016/j.epsl.2011.09.040, 2011.

Maloszewski, P. and Zuber, A.: Determining the turnover time of groundwater systems with the aid of environmental tracers, 1. Models and their applicability, J. Hydrol., 57, 207–231, 1982.

Maloszewski, P. and Zuber, A.: Principles and practice of calibration and validation of mathematical-models for the interpretation of environmental tracer data, Adv. Water Resour., 16, 173–190, doi:10.1016/0309-1708(93)90036-F, 1993.

Maloszewski, P., Maciejewski, S., Stumpp, C., Stichler, W., Trimborn, P., and Klotz, D.: Modelling of water flow through typical Bavarian soils: 2. Environmental deuterium transport, Hydrolog. Sci. J., 51, 298–313, doi:10.1623/hysj.51.2.298, 2006.

McDonnell, J. J.: Where does water go when it rains? Moving beyond the variable source area concept of rainfall–runoff response, Hydrol. Process., 17, 1869–1875, doi:10.1002/hyp.5132, 2003.

McDonnell, J. J., McGuire, K., Aggarwal, P., Beven, K. J., Biondi, D., Destouni, G., Dunn, S., James, A., Kirchner, J., Kraft, P., Lyon, S., Maloszewski, P., Newman, B., Pfister, L., Rinaldo, A., Rodhe, A., Sayama, T., Seibert, J., Solomon, K., Soulsby, C., Stewart, M., Tetzlaff, D., Tobin, C., Troch, P., Weiler, M., Western, A., Worman, A., and Wrede, S.: How old is streamwater? Open questions in catchment transit time conceptualization, modelling and analysis, Hydrol. Process., 24, 1745–1754, doi:10.1002/hyp.7796, 2010.

McGrane, S. J., Tetzlaff, D., and Soulsby, C.: Influence of lowland aquifers and anthropogenic impacts on the isotope hydrology of contrasting mesoscale catchments, Hydrol. Process., 28, 793–808, doi:10.1002/hyp.9610, 2014.

McGuire, K. J. and McDonnell, J. J.: A review and evaluation of catchment transit time modeling, J. Hydrol., 330, 543–563, doi:10.1016/j.jhydrol.2006.04.020, 2006.

HESSD
11, 12443–12488, 2014

Sampling frequency trade-offs in the assessment of mean transit times

E. Timbe et al.

CC BY

McGuire, K. J., DeWalle, D. R., and Gburek, W. J.: Evaluation of mean residence time in subsurface waters using oxygen-18 fluctuations during drought conditions in the mid-Appalachians, J. Hydrol., 261, 132–149, doi:10.1016/S0022-1694(02)00006-9, 2002.

McGuire, K. J., McDonnell, J. J., Weiler, M., Kendall, C., McGlynn, B. L., Welker, J. M., and Seibert, J.: The role of topography on catchment-scale water residence time, Water Resour. Res., 41, W05002, doi:10.1029/2004WR003657, 2005.

McGuire, K. J., Weiler, M., and McDonnell, J. J.: Integrating tracer experiments with modeling to assess runoff processes and water transit times, Adv. Water Resour., 30, 824–837, doi:10.1016/j.advwatres.2006.07.004, 2007.

Muñoz-Villers, L. E. and McDonnell, J. J.: Runoff generation in a steep, tropical montane cloud forest catchment on permeable volcanic substrate, Water Resour. Res., 48, W09528, doi:10.1029/2011WR011316, 2012.

Nash, J. E. and Sutcliffe, J. V.: River flow forecasting through conceptual models part I – a discussion of principles, J. Hydrol., 10, 282–290, doi:10.1016/0022-1694(70)90255-6, 1970.

Phillips, J. D.: Sources of nonlinearity and complexity in geomorphic systems, Prog. Phys. Geogr., 27, 1–23, doi:doi:10.1191/0309133303pp340ra, 2003.

Plesca, I., Timbe, E., Exbrayat, J.-F., Windhorst, D., Kraft, P., Crespo, P., Vache, K. B., Frede, H.-G., and Breuer, L.: Model intercomparison to explore catchment functioning: results from a remote montane tropical rainforest, Ecol. Model., 239, 3–13, doi:10.1016/j.ecolmodel.2011.05.005, 2012.

Rinaldo, A., Beven, K. J., Bertuzzo, E., Nicotina, L., Davies, J., Fiori, A., Russo, D., and Botter, G.: Catchment travel time distributions and water flow in soils, Water Resour. Res., 47, W07537, doi:10.1029/2011WR010478, 2011.

Rodgers, P., Soulsby, C., Waldron, S., and Tetzlaff, D.: Using stable isotope tracers to assess hydrological flow paths, residence times and landscape influences in a nested mesoscale catchment, Hydrol. Earth Syst. Sci., 9, 139–155, doi:10.5194/hess-9-139-2005, 2005.

Rollenbeck, R., Bendix, J., and Fabian, P.: Spatial and temporal dynamics of atmospheric water inputs in tropical mountain forests of South Ecuador, Hydrol. Process., 25, 344–352, doi:10.1002/hyp.7799, 2011.

Schumer, R., Benson, D. A., Meerschaert, M. M., and Baeumer, B.: Fractal mobile/immobile solute transport, Water Resour. Res., 39, 1296–1307, doi:10.1029/2003WR002141, 2003.

HESSD
11, 12443–12488, 2014

CC BY

Soulsby, C., Malcolm, R., Helliwell, R., Ferrier, R. C., and Jenkins, A.: Isotope hydrology of the Allt a' Mharcaidh catchment, Cairngorms, Scotland: implications for hydrological pathways and residence times, Hydrol. Process., 14, 747–762, doi:10.1002/(SICI)1099-1085(200003)14:4<747::AID-HYP970>3.0.CO;2-0, 2000.

Soulsby, C., Tetzlaff, D., and Hrachowitz, M.: Tracers and transit times: windows for viewing catchment scale storage?, Hydrol. Process., 23, 3503–3507, doi:10.1002/hyp.7501, 2009.

Soulsby, C., Tetzlaff, D., and Hrachowitz, M.: Are transit times useful process-based tools for flow prediction and classification in ungauged basins in montane regions?, Hydrol. Process., 24, 1685–1696, doi:10.1002/hyp.7578, 2010.

Speed, M., Tetzlaff, D., Soulsby, C., Hrachowitz, M., and Waldron, S.: Isotopic and geochemical tracers reveal similarities in transit times in contrasting mesoscale catchments, Hydrol. Process., 24, 1211–1224, doi:10.1002/hyp.7593, 2010.

Stewart, M. K., Morgenstern, U., and McDonnell, J. J.: Truncation of stream residence time: how the use of stable isotopes has skewed our concept of streamwater age and origin, Hydrol. Process., 24, 1646–1659, doi:10.1002/hyp.7576, 2010.

Timbe, E., Windhorst, D., Crespo, P., Frede, H.-G., Feyen, J., and Breuer, L.: Understanding uncertainties when inferring mean transit times of water trough tracer-based lumped-parameter models in Andean tropical montane cloud forest catchments, Hydrol. Earth Syst. Sci., 18, 1503–1523, doi:10.5194/hess-18-1503-2014, 2014.

Vaché, K. B. and McDonnell, J. J.: A process-based rejectionist framework for evaluating catchment runoff model structure, Water Resour. Res., 42, W02409, doi:10.1029/2005WR004247, 2006.

Viville, D., Ladouche, B., and Bariac, T.: Isotope hydrological study of mean transit time in the granitic Strengbach catchment (Vosges massif, France): application of the FlowPC model with modified input function, Hydrol. Process., 20, 1737–1751, doi:10.1002/hyp.5950, 2006.

Weiler, M., McGlynn, B. L., McGuire, K. J., and McDonnell, J. J.: How does rainfall become runoff? A combined tracer and runoff transfer function approach, Water Resour. Res., 39, 1315, doi:10.1029/2003WR002331, 2003.

Wilcke, W., Yasin, S., Schmitt, A., Valarezo, C., and Zech, W.: Soils along the altitudinal transect and in catchments, in: Gradients in a Tropical Mountain Ecosystem of Ecuador, edited by: Beck, E., Bendix, J., Kottke, I., Makeschin, F., and Mosandl, R., Springer, Berlin, 75–85, 2008.

HESSD
11, 12443–12488, 2014

CC BY

Willems, P.: A time series tool to support the multi-criteria performance evaluation of rainfall–runoff models, Environ. Model. Softw., 24, 311–321, doi:10.1016/j.envsoft.2008.09.005, 2009.

Windhorst, D., Waltz, T., Timbe, E., Frede, H.-G., and Breuer, L.: Impact of elevation and weather patterns on the isotopic composition of precipitation in a tropical montane rainforest, Hydrol. Earth Syst. Sci., 17, 409–419, doi:10.5194/hess-17-409-2013, 2013.

cc BY

Table 1. Characteristics of the San Francisco catchment and tributaries.

Parameter	Units	Outlet	Sub-catchment						
		PL	FH	QZ	QN	QR	QP	QM	QC
Catchment physical characteristics									
Drainage area	[km^2]	76.9	34.9	11.2	9.8	4.7	3.4	1.3	0.7
Mean elevation	[m a.s.l.]	2531	2615	2615	2591	2472	2447	2274	2290
Altitude	[m]	1325	1133	991	975	1424	975	772	516
Mean slope	[%]	63	63	63	60	69	67	57	56
Hydrological parameters									
Discharge	[mm]	2959	2691	–	1291	–	–	3315	2742
Baseflow	[mm]	2520	2152	–	1044	–	–	2118	2268
	[%]	85.2	80	–	80.8	–	–	63.9	82.7
Land use									
Forest	[%]	68	67	72	65	80	63	90	22
Sub-páramo	[%]	21	29	15	17	18	10	9	10
Pasture/Bracken	[%]	9	3	12	16	2	26	1	67
Others	[%]	2	1	1	2	0	1	0	1

Legend: PL = Planta (catchment outlet), FH = Francisco Head, QZ = Zurita, QN = Navidades, QR = Ramon, QP = Pastos, QM = Milagro, QC = Cruces.

HESSD
11, 12443–12488, 2014

Sampling frequency trade-offs in the assessment of mean transit times

E. Timbe et al.

CC BY

Table 2. Applied sampling strategy in the San Francisco catchment.

Sample type	Collection method	Sampled since[a]	Site name	Site code	Altitude m a.s.l.	Number of samples
Rainfall	Manually	Oct 2010	Estación San Francisco	ECSF	1900	946
Main river	Manually	Oct 2010	Planta (outlet)	PL	1725	104
Tributaries	Manually	Oct 2010	Francisco Head	FH	1917	98
			Zurita	QZ	2047	103
			Navidades	QN	2050	104
			Ramon	QR	1726	104
			Pastos	QP	1925	103
			Milagro	QM	1878	104
			Cruces	QR	1978	102
Pastures soil water	Wick-sampler[b]	Nov 2010	Pastos alto	A	2025	58
			Pastos medio	B	1975	70
			Pastos bajo	C	1925	71
Forest soil water	Wick-sampler[b]	Sep 2010	Bosque alto	D	2000	74
			Bosque medio	E	1900	80
			Bosque bajo	F	1825	53

[a] Sampling campaign was completed mid-Aug 2012.
[b] All wick-samplers are located at a depth of 0.25 m below surface.

HESSD
11, 12443–12488, 2014

CC BY

Table 3. Soil water simulation results using GM and LPM models considering type 1 scenarios.

Parameter	Sf	A_{GM}	B_{GM}	C_{GM}	D_{GM}	E_{GM}	F_{GM}	$\widetilde{X}_{GM}$	A_{LPM}	B_{LPM}	C_{LPM}	D_{LPM}	E_{LPM}	F_{LPM}	$\widetilde{X}_{LPM}$
τ	1	4.82	4.50	3.42	6.93	6.74	4.44	**4.66**	4.58	4.61	3.23	5.99	6.14	4.36	**4.59**
[weeks]	2	5.33	4.97	3.75	7.48	7.02	4.67	**5.15**	5.69	4.53	3.79	6.29	6.11	4.49	**5.11**
	3	6.01	5.41	4.56	8.43	8.26	5.77	**5.89**	5.96	5.18	4.27	7.71	7.34	5.92	**5.94**
	4	7.27	5.79	4.98	9.30	9.75	5.97	**6.62**	7.17	7.69	4.19	8.31	9.17	6.18	**7.43**
	5	9.68	8.22	7.55	9.74	10.58	8.29	**8.99**	11.02	8.87	8.87	8.75	8.17	11.60	**8.87**
$\Delta\tau$	1	2.05	1.62	1.68	2.03	1.58	1.98	**1.83**	1.64	1.43	1.67	1.12	1.25	1.44	**1.44**
[weeks]	2	2.08	1.92	1.69	2.17	1.95	1.89	**1.93**	1.75	1.27	1.52	1.43	1.52	1.75	**1.52**
	3	1.84	2.16	1.75	2.39	2.27	2.06	**2.11**	1.55	2.22	2.00	1.04	0.93	1.77	**1.66**
	4	1.62	1.93	1.49	2.40	2.55	1.82	**1.87**	1.60	1.48	3.07	1.59	1.65	1.43	**1.60**
	5	1.87	2.41	1.95	2.17	2.44	1.67	**2.06**	3.49	3.73	3.53	3.31	3.45	3.34	**3.47**
α or η	1	1.51	1.76	1.59	2.11	3.64	2.66	**1.94**	1.02	1.01	1.02	1.00	1.07	1.17	**1.02**
[–]	2	1.64	1.72	1.71	2.04	2.76	2.21	**1.88**	1.07	1.01	1.07	1.03	1.00	1.03	**1.03**
	3	1.85	1.97	3.11	1.93	2.37	1.78	**1.95**	1.01	1.03	1.02	1.08	1.02	1.19	**1.03**
	4	3.91	4.75	5.06	2.73	2.32	3.55	**3.73**	1.16	1.22	1.00	1.01	1.12	1.02	**1.07**
	5	4.50	4.86	6.19	4.58	3.94	4.52	**4.55**	1.40	1.15	1.12	1.08	1.03	1.51	**1.14**
Δ_α or Δ_η	1	2.83	3.02	2.95	2.70	5.64	6.72	**2.99**	0.17	0.36	0.37	0.27	0.39	0.59	**0.36**
[–]	2	1.69	2.65	3.69	1.76	3.53	3.56	**3.09**	0.09	0.34	0.51	0.23	0.45	0.39	**0.37**
	3	1.98	2.96	4.89	1.51	2.11	2.14	**2.13**	0.16	0.18	1.16	0.12	0.14	0.17	**0.17**
	4	2.86	4.07	3.26	1.92	1.23	3.51	**3.06**	0.30	0.26	0.39	0.21	0.21	0.27	**0.27**
	5	1.92	4.01	6.28	2.11	1.94	3.38	**2.75**	0.46	0.48	0.45	0.44	0.44	0.44	**0.45**
NSE	1	0.69	0.76	0.86	0.83	0.78	0.88	**0.81**	0.70	0.76	0.85	0.82	0.78	0.88	**0.80**
[–]	2	0.74	0.81	0.89	0.87	0.82	0.94	**0.84**	0.74	0.80	0.88	0.84	0.81	0.92	**0.83**
	3	0.81	0.84	0.90	0.88	0.79	0.91	**0.86**	0.81	0.81	0.90	0.83	0.78	0.87	**0.82**
	4	0.78	0.88	0.87	0.80	0.64	0.92	**0.84**	0.77	0.87	0.84	0.72	0.58	0.89	**0.81**
	5	0.66	0.83	0.83	0.87	0.76	0.82	**0.83**	0.67	0.78	0.73	0.85	0.70	0.79	**0.76**
RMSE	1	1.85	1.65	1.28	1.06	1.36	1.10	**1.32**	1.81	1.65	1.35	1.10	1.35	1.10	**1.35**
[‰]	2	1.67	1.46	1.14	0.93	1.24	0.79	**1.19**	1.67	1.50	1.21	1.03	1.26	0.87	**1.23**
	3	1.36	1.41	1.05	0.89	1.31	0.86	**1.18**	1.36	1.51	1.08	1.02	1.33	1.05	**1.20**
	4	1.29	1.04	1.13	1.07	1.59	0.78	**1.10**	1.32	1.09	1.28	1.26	1.72	0.94	**1.27**
	5	1.42	1.11	1.28	0.80	1.20	1.05	**1.16**	1.42	1.25	1.60	0.86	1.35	1.13	**1.30**
BIAS	1	0.34	0.03	−0.06	0.10	−0.09	0.23	**0.07**	0.22	0.00	−0.15	0.03	−0.06	0.11	**0.02**
[‰]	2	0.21	−0.06	−0.28	−0.02	−0.14	0.14	**−0.04**	−0.04	−0.03	−0.10	0.11	−0.03	−0.02	**−0.03**
	3	−0.01	−0.20	−0.39	−0.11	−0.20	−0.07	**−0.16**	−0.07	−0.01	0.03	0.07	0.00	0.08	**0.02**
	4	−0.17	−0.30	−0.07	−0.24	−0.13	−0.16	**−0.16**	0.05	−0.07	0.07	0.08	0.12	−0.05	**0.06**
	5	0.11	−0.09	−0.13	−0.07	−0.05	−0.08	**−0.08**	0.03	−0.07	−0.17	−0.01	0.03	−0.05	**−0.03**

Sf = Sampling frequency or time resolution of data: 1 = daily data for rainfall and weekly data for soil water, 2 = weekly data for rainfall and soil water, 3 = biweekly data for rainfall and soil water, 4 = monthly data for rainfall and soil water, 5 = bimonthly data for rainfall and soil water; A, B and C = pasture soil water sites located at 2025, 1975 and 1925 m a.s.l.; D-F = soil water sites located at 2000, 1900 and 1825 m a.s.l. The subscript of the names of the soil site are related to the lumped model used: GM = Gamma, LPM = Linear Piston Flow; $\widetilde{X}$ = median of results of soil sites per sampling frequency; τ and $\Delta\tau$ = tracer's mean transit time (best match) and its corresponding uncertainty range length; α and Δ_α for GM (or η and Δ_η for LPM) = best matching result for the second lumped parameter and corresponding uncertainty range length; NSE = Nash–Sutcliffe Efficiency of best match; RMSE = Root Mean Square Error.

HESSD
11, 12443–12488, 2014
Sampling frequency trade-offs in the assessment of mean transit times
E. Timbe et al.

cc BY

Table 4. Soil water simulation results using GM and LPM models considering type 2 scenarios.

Parameter	Sr	A_{GM}	B_{GM}	C_{GM}	D_{GM}	E_{GM}	F_{GM}	$\widetilde{X}_{GM}$	A_{LPM}	B_{LPM}	C_{LPM}	D_{LPM}	E_{LPM}	F_{LPM}	$\widetilde{X}_{LMP}$
τ [weeks]	1	4.82	4.50	3.42	6.93	6.74	4.44	**4.66**	4.58	4.61	3.23	5.99	6.14	4.36	**4.59**
	2	5.33	4.97	3.75	7.48	7.02	4.67	**5.15**	5.69	4.53	3.79	6.29	6.11	4.49	**5.11**
	3	5.50	4.99	3.88	7.67	7.21	4.81	**5.25**	5.80	4.88	3.64	6.88	6.89	4.81	**5.34**
	4	5.57	5.01	3.95	7.75	7.24	4.49	**5.29**	5.77	4.72	3.86	6.73	6.88	4.46	**5.25**
	5	5.38	4.16	2.69	6.46	6.37	4.63	**5.00**	4.99	3.92	2.83	5.62	6.17	4.37	**4.68**
$\Delta\tau$ [weeks]	1	2.05	1.62	1.68	2.03	1.58	1.98	**1.83**	1.64	1.43	1.67	1.12	1.25	1.44	**1.44**
	2	2.08	1.92	1.69	2.17	1.95	1.89	**1.93**	1.75	1.27	1.52	1.43	1.52	1.75	**1.52**
	3	2.11	2.04	1.79	2.07	2.07	1.97	**2.06**	1.45	1.35	1.61	1.00	1.31	1.73	**1.40**
	4	1.87	1.91	1.77	2.52	2.05	1.81	**1.89**	1.53	1.66	1.81	0.89	1.41	1.74	**1.60**
	5	1.74	2.30	1.93	2.20	1.84	1.80	**1.89**	1.35	1.72	2.04	1.60	1.79	1.28	**1.66**
α or η [–]	1	1.51	1.76	1.59	2.11	3.64	2.66	**1.94**	1.02	1.01	1.02	1.00	1.07	1.17	**1.02**
	2	1.64	1.72	1.71	2.04	2.76	2.21	**1.88**	1.07	1.01	1.07	1.03	1.00	1.03	**1.03**
	3	1.70	1.61	1.53	1.76	2.32	1.83	**1.73**	1.08	1.08	1.02	1.05	1.06	1.08	**1.07**
	4	1.85	2.38	2.26	1.87	2.31	2.19	**2.23**	1.06	1.04	1.08	1.00	1.06	1.02	**1.05**
	5	2.31	1.42	1.37	1.91	3.71	1.65	**1.78**	1.07	1.03	1.17	1.03	1.26	1.04	**1.06**
Δ_α or Δ_η [–]	1	2.83	3.02	2.95	2.70	5.64	6.72	**2.99**	0.17	0.36	0.37	0.27	0.39	0.59	**0.36**
	2	1.69	2.65	3.69	1.76	3.53	3.56	**3.09**	0.09	0.34	0.51	0.23	0.45	0.39	**0.37**
	3	1.90	2.41	4.05	1.40	2.59	3.47	**2.50**	0.24	0.34	0.54	0.18	0.25	0.39	**0.29**
	4	2.42	5.39	6.35	1.69	2.80	5.95	**4.10**	0.29	0.73	1.16	0.17	0.25	0.92	**0.51**
	5	18.82	2.41	2.45	3.31	9.09	5.19	**4.25**	0.64	0.42	1.18	0.47	0.92	0.41	**0.56**
NSE [–]	1	0.69	0.76	0.86	0.83	0.78	0.88	**0.81**	0.70	0.76	0.85	0.82	0.78	0.88	**0.80**
	2	0.74	0.81	0.89	0.87	0.82	0.94	**0.84**	0.74	0.80	0.88	0.84	0.81	0.92	**0.83**
	3	0.73	0.82	0.89	0.86	0.82	0.93	**0.84**	0.73	0.80	0.88	0.82	0.82	0.90	**0.82**
	4	0.68	0.82	0.88	0.79	0.76	0.91	**0.81**	0.68	0.82	0.87	0.77	0.75	0.89	**0.80**
	5	0.64	0.71	0.77	0.84	0.79	0.81	**0.78**	0.69	0.70	0.75	0.82	0.79	0.83	**0.77**
RMSE [‰]	1	1.85	1.65	1.28	1.06	1.36	1.10	**1.32**	1.81	1.65	1.35	1.10	1.35	1.10	**1.35**
	2	1.67	1.46	1.14	0.93	1.24	0.79	**1.19**	1.67	1.50	1.21	1.03	1.26	0.87	**1.23**
	3	1.71	1.43	1.12	0.96	1.22	0.85	**1.17**	1.71	1.52	1.22	1.09	1.25	1.00	**1.24**
	4	1.88	1.42	1.21	1.19	1.44	0.96	**1.31**	1.88	1.42	1.25	1.24	1.46	1.03	**1.33**
	5	2.00	1.84	1.67	1.04	1.34	1.37	**1.52**	1.85	1.87	1.75	1.09	1.34	1.30	**1.54**
BIAS [‰]	1	0.34	0.03	−0.06	0.10	−0.09	0.23	**0.07**	0.22	0.00	−0.15	0.03	−0.06	0.11	**0.02**
	2	0.21	−0.06	−0.28	−0.02	−0.14	0.14	**−0.04**	−0.04	−0.03	−0.10	0.11	−0.03	−0.02	**−0.03**
	3	0.16	−0.14	−0.20	0.00	0.01	0.10	**0.01**	−0.03	−0.03	0.03	0.04	−0.02	0.09	**0.00**
	4	0.07	−0.28	−0.32	−0.22	0.03	0.13	**−0.10**	−0.04	−0.14	−0.09	0.00	−0.01	−0.05	**−0.05**
	5	0.43	0.23	0.10	0.00	0.07	0.36	**0.17**	−0.04	−0.04	0.07	0.00	−0.07	−0.04	**−0.04**

Sf = Sampling frequency or time resolution of data: 1 = daily data for rainfall and weekly data for soil water, 2 = weekly data for rainfall and soil water, 3 = biweekly data for rainfall and weekly data for soil water, 4 = monthly data for rainfall and weekly data for soil water, 5 = bimonthly data for rainfall and weekly data for soil water; A, B and C = pasture soil water sites located at 2025, 1975 and 1925 m a.s.l.; D-F = soil water sites located at 2000, 1900 and 1825 m a.s.l. The subscript of the names of the soil site are related to the lumped model used: GM = Gamma, LPM = Linear Piston Flow; $\widetilde{X}$ = median of results of soil sites per sampling frequency; τ and $\Delta\tau$ = tracer's mean transit time (best match) and its corresponding uncertainty range length; α and Δ_α for GM (or η and Δ_η for LPM) = best matching result for the second lumped parameter and corresponding uncertainty range length; NSE = Nash–Sutcliffe Efficiency of best match; RMSE = Root Mean Square Error.

HESSD
11, 12443–12488, 2014

Table 5. Stream water simulation results using GM and EPM models considering type 1 scenarios.

Parameter	Sf	PL_{GM}	FH_{GM}	QC_{GM}	QM_{GM}	QN_{GM}	QP_{GM}	QR_{GM}	QZ_{GM}	$\widetilde{X}_{GM}$	PL_{EPM}	FH_{EPM}	QC_{EPM}	QM_{EPM}	QN_{EPM}	QP_{EPM}	QR_{EPM}	QZ_{EPM}	$\widetilde{X}_{EPM}$
τ	1	1.98	1.62	4.16	1.99	1.56	3.91	3.13	2.22	**2.10**	2.61	2.68	3.33	2.59	2.67	3.24	2.76	2.74	**2.71**
[yr]	2	1.86	1.58	4.20	1.88	1.65	3.68	3.13	2.05	**1.97**	2.72	2.81	3.52	2.74	2.82	3.41	2.89	2.94	**2.86**
	3	1.55	1.34	4.07	1.40	1.43	3.12	2.36	1.61	**1.58**	2.78	2.87	3.68	2.70	2.86	3.53	2.95	2.89	**2.88**
	4	1.52	1.60	3.59	1.57	1.39	2.40	2.38	1.61	**1.61**	3.03	3.23	4.89	3.00	3.05	3.82	3.28	3.21	**3.22**
	5	1.16	1.23	2.22	1.08	1.24	1.95	1.63	1.23	**1.23**	2.90	2.94	5.56	2.82	3.01	3.68	3.19	3.06	**3.03**
$\Delta\tau$	1	1.62	1.44	1.69	2.12	1.36	1.96	1.80	1.89	**1.74**	0.25	0.26	0.36	0.25	0.26	0.43	0.31	0.31	**0.28**
[yr]	2	1.43	1.25	1.59	1.52	1.30	1.94	1.84	1.66	**1.56**	0.27	0.31	0.52	0.29	0.30	0.50	0.32	0.33	**0.32**
	3	1.13	0.92	1.48	1.18	0.92	1.81	1.62	1.12	**1.16**	0.29	0.31	0.58	0.28	0.32	0.51	0.31	0.31	**0.31**
	4	0.99	0.96	1.95	1.05	0.77	1.63	1.61	1.01	**1.03**	0.35	0.38	0.64	0.34	0.32	0.55	0.48	0.36	**0.37**
	5	0.51	0.62	1.14	0.53	0.52	0.93	0.88	0.55	**0.58**	0.30	0.36	0.62	0.30	0.34	0.62	0.45	0.38	**0.37**
α or η	1	0.57	0.68	0.63	0.55	0.67	0.63	0.54	0.62	**0.63**	3.14	3.10	2.15	3.23	3.09	2.23	2.79	2.93	**3.01**
[–]	2	0.63	0.73	0.65	0.60	0.70	0.67	0.60	0.68	**0.66**	2.97	2.89	2.05	2.92	2.89	2.14	2.66	2.63	**2.77**
	3	0.70	0.79	0.68	0.68	0.76	0.74	0.67	0.74	**0.72**	2.96	2.91	1.96	3.14	2.81	2.09	2.59	2.75	**2.78**
	4	0.79	0.87	0.78	0.77	0.88	0.88	0.74	0.87	**0.83**	2.73	2.46	2.37	2.77	2.69	2.00	2.26	2.48	**2.47**
	5	0.93	0.93	0.93	0.92	0.98	0.98	0.88	0.99	**0.93**	2.73	2.65	2.94	2.87	2.56	1.99	2.35	2.50	**2.60**
Δ_α or Δ_η	1	0.16	0.20	0.09	0.14	0.19	0.11	0.10	0.15	**0.14**	0.68	0.60	0.27	0.69	0.59	0.35	0.45	0.60	**0.59**
[–]	2	0.15	0.19	0.10	0.15	0.17	0.13	0.11	0.17	**0.15**	0.57	0.55	0.30	0.64	0.55	0.36	0.48	0.53	**0.54**
	3	0.16	0.21	0.09	0.16	0.19	0.16	0.13	0.18	**0.16**	0.58	0.58	0.28	0.64	0.54	0.32	0.45	0.48	**0.51**
	4	0.19	0.21	0.14	0.18	0.20	0.22	0.16	0.22	**0.19**	0.50	0.43	0.41	0.48	0.43	0.27	0.40	0.41	**0.42**
	5	0.18	0.16	0.18	0.18	0.19	0.20	0.15	0.19	**0.18**	0.48	0.54	0.60	0.53	0.45	0.32	0.42	0.44	**0.46**
NSE	1	0.63	0.56	0.59	0.60	0.70	0.57	0.50	0.63	**0.60**	0.59	0.55	0.62	0.54	0.66	0.61	0.49	0.63	**0.60**
[–]	2	0.60	0.58	0.58	0.57	0.66	0.56	0.46	0.60	**0.58**	0.59	0.56	0.62	0.54	0.64	0.61	0.54	0.62	**0.60**
	3	0.68	0.62	0.66	0.67	0.72	0.63	0.54	0.71	**0.66**	0.62	0.57	0.67	0.60	0.69	0.64	0.62	0.70	**0.63**
	4	0.71	0.60	0.73	0.75	0.79	0.76	0.72	0.79	**0.74**	0.65	0.58	0.83	0.66	0.77	0.74	0.70	0.77	**0.72**
	5	0.76	0.73	0.78	0.80	0.78	0.80	0.81	0.85	**0.79**	0.75	0.72	0.77	0.78	0.78	0.80	0.78	0.85	**0.78**
RMSE	1	0.33	0.35	0.19	0.38	0.27	0.22	0.34	0.28	**0.31**	0.35	0.35	0.19	0.40	0.29	0.21	0.34	0.28	**0.32**
[‰]	2	0.35	0.34	0.20	0.39	0.29	0.22	0.36	0.30	**0.32**	0.35	0.35	0.19	0.40	0.30	0.21	0.33	0.29	**0.31**
	3	0.31	0.34	0.16	0.35	0.27	0.19	0.33	0.26	**0.29**	0.34	0.36	0.16	0.38	0.28	0.19	0.30	0.26	**0.29**
	4	0.26	0.29	0.13	0.25	0.21	0.14	0.20	0.18	**0.20**	0.29	0.30	0.11	0.28	0.22	0.14	0.21	0.19	**0.21**
	5	0.22	0.23	0.12	0.21	0.19	0.11	0.15	0.14	**0.17**	0.22	0.23	0.12	0.21	0.19	0.11	0.16	0.14	**0.17**
BIAS	1	0.05	0.02	0.03	0.06	0.02	0.02	0.06	0.03	**0.03**	0.02	0.01	0.00	0.01	0.00	0.01	0.02	0.00	**0.01**
[‰]	2	0.09	0.04	0.05	0.10	0.05	0.04	0.08	0.06	**0.05**	0.01	0.00	0.00	0.02	0.00	0.01	0.00	0.01	**0.00**
	3	0.09	0.06	0.04	0.10	0.07	0.04	0.09	0.07	**0.07**	0.00	0.00	0.00	0.00	0.00	0.00	−0.01	0.00	**0.00**
	4	0.07	0.03	0.04	0.08	0.03	0.02	0.07	0.03	**0.03**	0.00	−0.01	0.00	0.00	−0.01	0.00	0.00	0.00	**0.00**
	5	0.05	0.02	0.03	0.06	0.02	0.01	0.05	0.01	**0.03**	−0.01	0.00	0.00	0.00	0.00	0.00	0.01	0.00	**0.00**

Sf = Sampling frequency or time resolution of data: 1 = daily frequency for rainfall and weekly for stream water, 2 = weekly frequency for rainfall and stream water, 3 = biweekly frequency for rainfall and stream water, 4 = monthly frequency for rainfall and stream water, 5 = bimonthly frequency for rainfall and stream water. Acronyms for stream water are defined in Fig. 1 and the subscripts for stream water sites stands for the lumped model used: GM = Gamma, EPM = Exponential Piston Flow. $\widetilde{X}$ = median of the results of stream water sites per sampling frequency; τ and $\Delta\tau$ = tracer's mean transit time (best match) and its corresponding uncertainty range length; α and Δ_α for GM (or η and Δ_η for EPM) = the best matching result for the second lumped parameter and corresponding uncertainty range length; NSE = Nash–Sutcliffe Efficiency of best match; RMSE = Root Mean Square Error.

HESSD

11, 12443–12488, 2014

Table 6. Stream water simulation results using GM and EPM models considering type 2 scenarios.

Parameter	Tr	PL_{GM}	FH_{GM}	QC_{GM}	QM_{GM}	QN_{GM}	QP_{GM}	QR_{GM}	QZ_{GM}	$\widetilde{X}_{GM}$	PL_{EPM}	FH_{EPM}	QC_{EPM}	QM_{EPM}	QN_{EPM}	QP_{EPM}	QR_{EPM}	QZ_{EPM}	$\widetilde{X}_{EMP}$
τ	1	1.98	1.62	4.16	1.99	1.56	3.91	3.13	2.22	**2.10**	2.61	2.68	3.33	2.59	2.67	3.24	2.76	2.74	**2.71**
[yr]	2	1.86	1.58	4.20	1.88	1.65	3.68	3.13	2.05	**1.97**	2.72	2.81	3.52	2.74	2.82	3.41	2.89	2.94	**2.86**
	3	1.94	1.69	4.26	1.96	1.71	3.75	3.13	2.22	**2.09**	2.78	2.89	3.79	2.77	2.88	3.55	3.00	2.96	**2.93**
	4	2.50	2.45	5.58	2.55	2.12	5.43	3.81	2.75	**2.65**	2.85	2.04	2.75	2.79	2.87	3.56	3.06	2.96	**2.86**
	5	1.58	1.41	3.53	1.63	1.44	2.91	2.71	1.77	**1.70**	2.70	2.67	3.41	2.63	2.77	3.35	2.86	2.90	**2.81**
$\Delta\tau$	1	1.62	1.44	1.69	2.12	1.36	1.96	1.80	1.89	**1.74**	0.25	0.26	0.36	0.25	0.26	0.43	0.31	0.31	**0.28**
[yr]	2	1.43	1.25	1.59	1.52	1.30	1.94	1.84	1.66	**1.56**	0.27	0.31	0.52	0.29	0.30	0.50	0.32	0.33	**0.32**
	3	1.58	1.37	1.58	1.61	1.44	1.86	1.63	1.71	**1.59**	0.29	0.33	0.49	0.28	0.33	0.50	0.36	0.37	**0.35**
	4	2.08	2.36	1.41	2.13	2.02	1.71	1.98	2.47	**2.05**	0.28	0.37	0.56	0.26	0.25	0.33	0.28	0.28	**0.28**
	5	1.05	0.77	1.18	1.17	0.93	1.39	1.47	1.09	**1.13**	0.27	0.30	0.48	0.23	0.26	0.46	0.31	0.30	**0.30**
α or η	1	0.57	0.68	0.63	0.55	0.67	0.63	0.54	0.62	**0.63**	3.14	3.10	2.15	3.23	3.09	2.23	2.79	2.93	**3.01**
[–]	2	0.63	0.73	0.65	0.60	0.70	0.67	0.60	0.68	**0.66**	2.97	2.89	2.05	2.92	2.89	2.14	2.66	2.63	**2.77**
	3	0.62	0.71	0.66	0.60	0.69	0.68	0.60	0.67	**0.66**	2.85	2.76	1.91	2.86	2.77	2.06	2.47	2.60	**2.68**
	4	0.56	0.62	0.60	0.53	0.63	0.60	0.54	0.59	**0.60**	2.75	1.78	1.46	2.85	2.77	2.03	2.42	2.62	**2.52**
	5	0.65	0.73	0.70	0.64	0.73	0.75	0.64	0.72	**0.71**	3.05	3.17	2.11	3.20	2.95	2.18	2.67	2.67	**2.81**
Δ_α or Δ_η	1	0.16	0.20	0.09	0.14	0.19	0.11	0.10	0.15	**0.14**	0.68	0.60	0.27	0.69	0.59	0.35	0.45	0.60	**0.59**
[–]	2	0.15	0.19	0.10	0.15	0.17	0.13	0.11	0.17	**0.15**	0.57	0.55	0.30	0.64	0.55	0.36	0.48	0.53	**0.54**
	3	0.14	0.19	0.09	0.15	0.17	0.13	0.11	0.16	**0.15**	0.54	0.51	0.29	0.56	0.55	0.29	0.43	0.52	**0.51**
	4	0.13	0.17	0.07	0.13	0.17	0.07	0.08	0.16	**0.13**	0.52	0.24	0.13	0.52	0.43	0.24	0.35	0.39	**0.37**
	5	0.13	0.15	0.09	0.14	0.15	0.12	0.11	0.15	**0.14**	0.69	0.62	0.32	0.62	0.52	0.37	0.50	0.50	**0.51**
NSE	1	0.63	0.56	0.59	0.60	0.70	0.57	0.50	0.63	**0.60**	0.59	0.55	0.62	0.54	0.66	0.61	0.49	0.63	**0.60**
[–]	2	0.60	0.58	0.58	0.57	0.66	0.56	0.46	0.60	**0.58**	0.59	0.56	0.62	0.54	0.64	0.61	0.54	0.62	**0.60**
	3	0.59	0.56	0.56	0.56	0.65	0.53	0.45	0.60	**0.56**	0.55	0.52	0.58	0.51	0.61	0.56	0.51	0.59	**0.56**
	4	0.58	0.49	0.54	0.56	0.62	0.53	0.51	0.58	**0.55**	0.49	0.50	0.53	0.46	0.57	0.53	0.47	0.55	**0.51**
	5	0.47	0.47	0.36	0.43	0.52	0.36	0.34	0.45	**0.44**	0.56	0.53	0.56	0.52	0.57	0.51	0.49	0.54	**0.54**
RMSE	1	0.33	0.35	0.19	0.38	0.27	0.22	0.34	0.28	**0.31**	0.35	0.35	0.19	0.40	0.29	0.21	0.34	0.28	**0.32**
[‰]	2	0.35	0.34	0.20	0.39	0.29	0.22	0.36	0.30	**0.32**	0.35	0.35	0.19	0.40	0.30	0.21	0.33	0.29	**0.31**
	3	0.35	0.35	0.20	0.39	0.30	0.23	0.36	0.30	**0.32**	0.37	0.37	0.20	0.41	0.31	0.22	0.34	0.30	**0.33**
	4	0.36	0.38	0.21	0.39	0.31	0.23	0.34	0.30	**0.32**	0.39	0.37	0.21	0.44	0.33	0.23	0.36	0.31	**0.34**
	5	0.40	0.38	0.24	0.45	0.35	0.27	0.40	0.35	**0.36**	0.37	0.36	0.20	0.41	0.33	0.23	0.35	0.32	**0.34**
BIAS	1	0.05	0.02	0.03	0.06	0.02	0.02	0.06	0.03	**0.03**	0.02	0.01	0.00	0.01	0.00	0.01	0.02	0.00	**0.01**
[‰]	2	0.09	0.04	0.05	0.10	0.05	0.04	0.08	0.06	**0.05**	0.01	0.00	0.00	0.02	0.00	0.01	0.00	0.01	**0.00**
	3	0.09	0.04	0.04	0.10	0.05	0.03	0.08	0.05	**0.05**	0.00	0.01	−0.01	−0.01	−0.01	0.00	0.00	0.00	**0.00**
	4	0.04	−0.02	0.01	0.04	−0.02	0.00	0.03	0.00	**0.00**	−0.01	−0.02	−0.06	−0.01	−0.02	−0.05	−0.02	−0.02	**−0.02**
	5	0.15	0.11	0.10	0.15	0.11	0.09	0.13	0.11	**0.11**	0.01	−0.01	0.02	0.00	0.00	0.02	0.02	0.00	**0.00**

Sf = Sampling frequency or time resolution of data: 1 = daily frequency for rainfall and weekly for stream water, 2 = weekly frequency for rainfall and stream water, 3 = biweekly frequency for rainfall and weekly frequency for stream water, 4 = monthly frequency for rainfall and weekly frequency for stream water, 5 = bimonthly frequency for rainfall and weekly frequency for stream water. Acronyms for stream water are defined in Fig. 1 and the subscripts for stream water sites stands for the lumped model used: GM = Gamma, EPM = Exponential Piston Flow. $\widetilde{X}$ = median of the results of stream water sites per sampling frequency; τ and $\Delta\tau$ = tracer's mean transit time (best match) and its corresponding uncertainty range length; α and Δ_α for GM (or η and Δ_η for EPM) = the best matching result for the second lumped parameter and corresponding uncertainty range length; NSE = Nash–Sutcliffe Efficiency of best match; RMSE = Root Mean Square Error.

HESSD

11, 12443–12488, 2014

HESSD

11, 12443–12488, 2014

CC BY

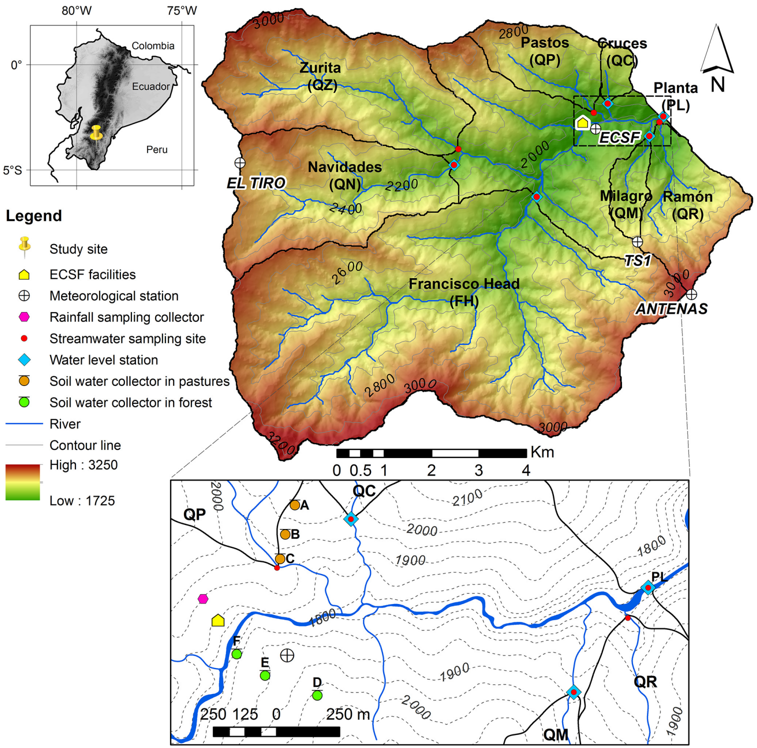

Figure 1. San Francisco catchment with sampling locations and delineation of corresponding drainage area. Names and acronyms are showed in bold. Framed image shows the zoomed area of the lower part of the catchment.

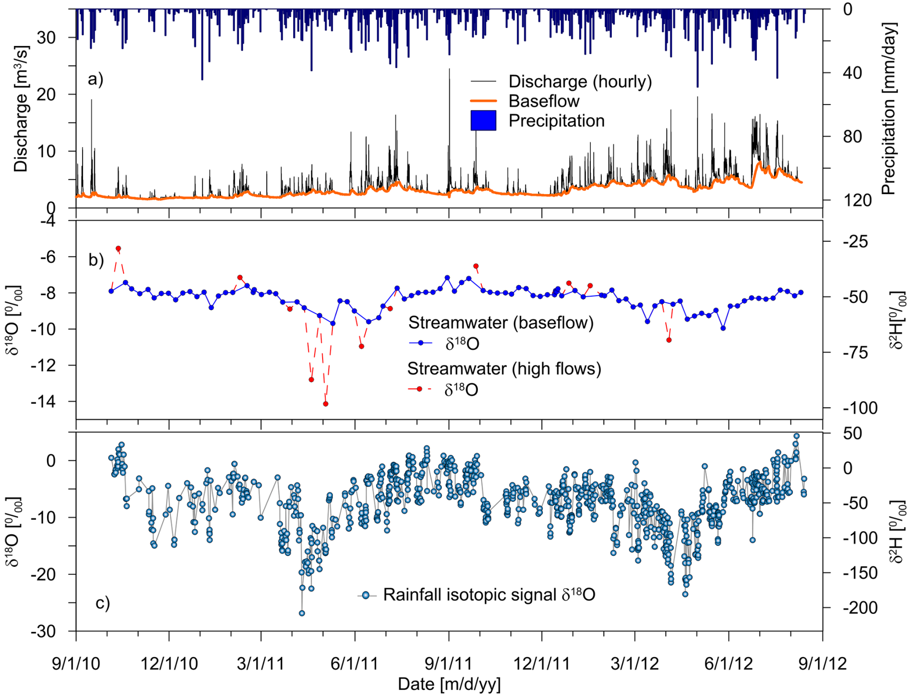

Figure 2. (a) Rainfall time series for ECSF meteorological station, hourly discharge and baseflow at the catchment outlet (PL); **(b)** weekly δ^{18}O and δ^{2}H of stream water at PL for baseflow and high flow conditions; and **(c)** light blue dots indicate δ^{18}O and δ^{2}H signatures.

HESSD
11, 12443–12488, 2014

Sampling frequency trade-offs in the assessment of mean transit times

E. Timbe et al.

CC BY

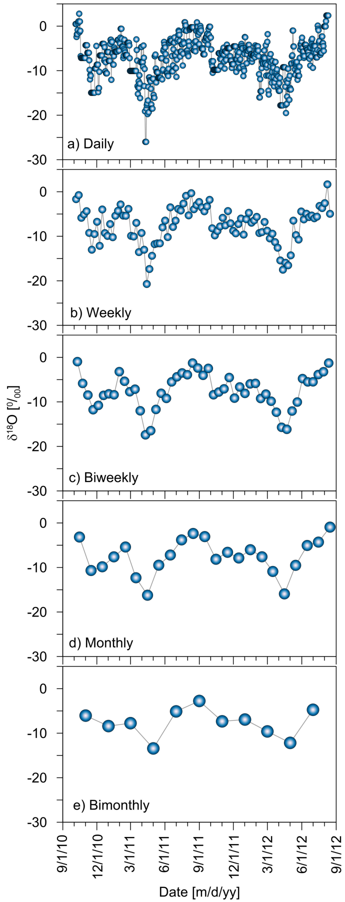

Figure 3. Data aggregation of observed $\delta^{18}O$ signatures of rainfall at ECSF (1900 m a.s.l.) into five levels of temporal data resolutions. Estimates were weighted according to the corresponding measured volume for every sample relative to the total volume of the time span.

HESSD

11, 12443–12488, 2014

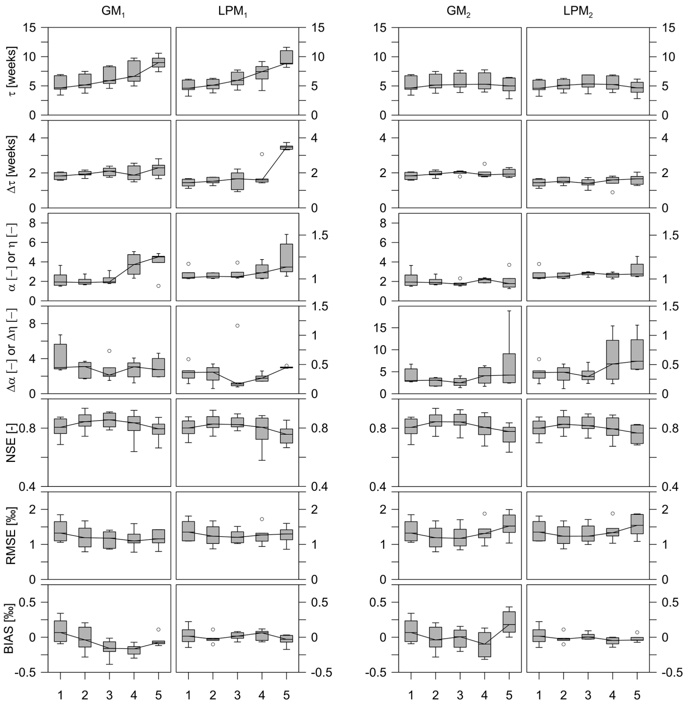

Figure 4. Comparison of predictions for soil water sites using GM and LPM lumped models. Subscript in the model name stands for the type of scenario: S1 = Aggregation of sampling frequency in the rainfall and also in the effluent, S2 = Aggregation of sampling frequency only in rainfall data. Values 1–5 in the x axis of all plots stands for five types of data resolution: 1 = Daily, 2 = Weekly; 3 = Biweekly, 4 = Monthly and 5 = Bimonthly. Box-plots markers correspond to quartiles and median values (–). The length of Whiskers is limited to 1.5 times the width of the box and values located further away below the first quartile or above the third quartile are considered extreme ones (◯).

HESSD
11, 12443–12488, 2014

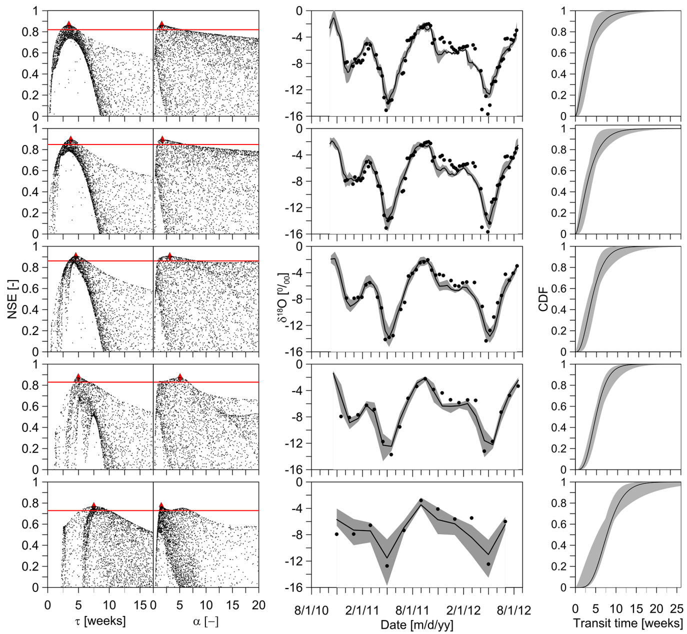

Figure 5. Predicted results for the soil water site C using the GM lumped model. Results are ranged from top to bottom according to the data resolution: daily (top), weekly, biweekly, monthly and bimonthly (bottom). Left column shows dotty plots for the model parameters (τ and α) according to NSE using Monte Carlo random simulations (GLUE approach). Red line shows the feasible range of behavioral solutions of model parameters as a 5 % of the top best prediction (red diamond). Center column shows the measured (black filled circles) and simulated $\delta^{18}O$ (the black line and the shaded area represent the best possible solution and its range of variation according to the 5–95 % of weighted quantiles derived from the confidence limits of behavioral solutions shown in the left column. Right column: soil water residence time distribution function corresponding to the best NSE; gray shaded area in each plot corresponds to the range of possible shapes of the distribution function.

HESSD
11, 12443–12488, 2014

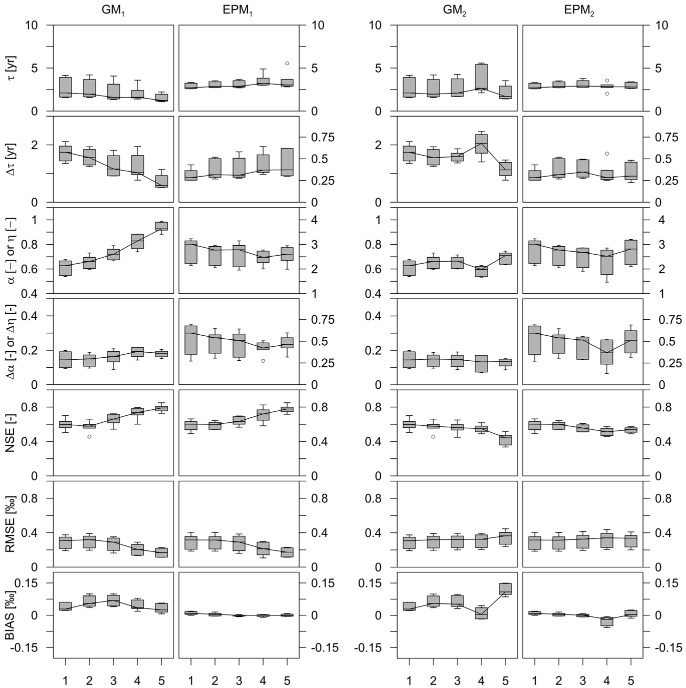

Figure 6. Comparison of predictions for stream water sites using the GM and EPM lumped models. The subscript in the model name stands for the type of scenario: S1 = Aggregation of sampling frequency in the rainfall and also in the effluent, S2 = Aggregation of sampling frequency only in rainfall data. Values 1–5 in the *x* axis of all plots stands for five types of data resolution: 1 = Daily, 2 = Weekly; 3 = Biweekly, 4 = Monthly and 5 = Bimonthly. Box-plots markers correspond to quartiles and median values are shown (–). The length of Whiskers is limited to 1.5 times the width of the box and values located further away below the first quartile or above the third quartile are considered extreme ones (◯).

HESSD
11, 12443–12488, 2014

Sampling frequency trade-offs in the assessment of mean transit times

E. Timbe et al.

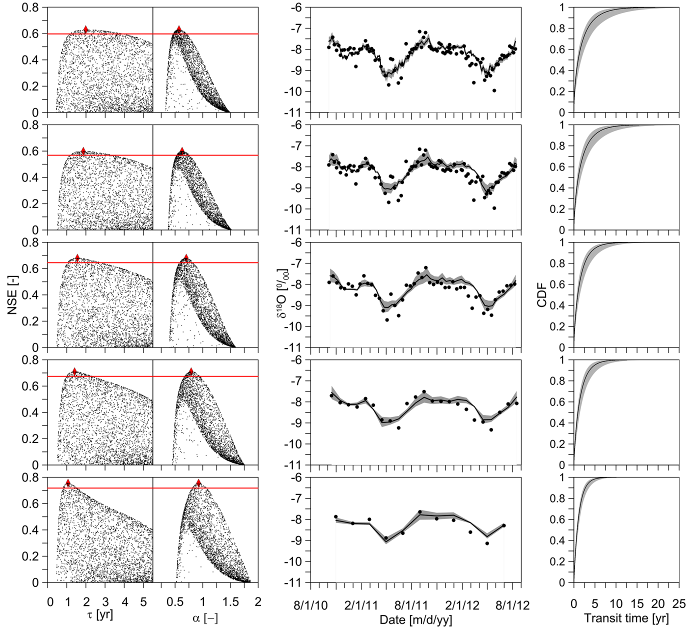

Figure 7. Predicted results for the stream water site PL using the GM lumped model. Results are ranged from top to bottom according to the data resolution: daily (top), weekly, biweekly, monthly and bimonthly (bottom). Left column shows dotty plots for the model parameters (τ and α) according to NSE using Monte Carlo random simulations (GLUE approach). Red line shows the feasible range of behavioral solutions of model parameters as a 5 % of the top best prediction (red diamond). Center column shows the measured (black filled circles) and simulated δ^{18}O (the black line and the shaded area represent the best possible solution and its range of variation according to the 5–95 % of weighted quantiles derived from the confidence limits of behavioral solutions shown in the left column. Right column: soil water residence time distribution function corresponding to the best NSE; gray shaded area in each plot corresponds to the range of possible shapes of the distribution function.

HESSD
11, 12443–12488, 2014

CC BY

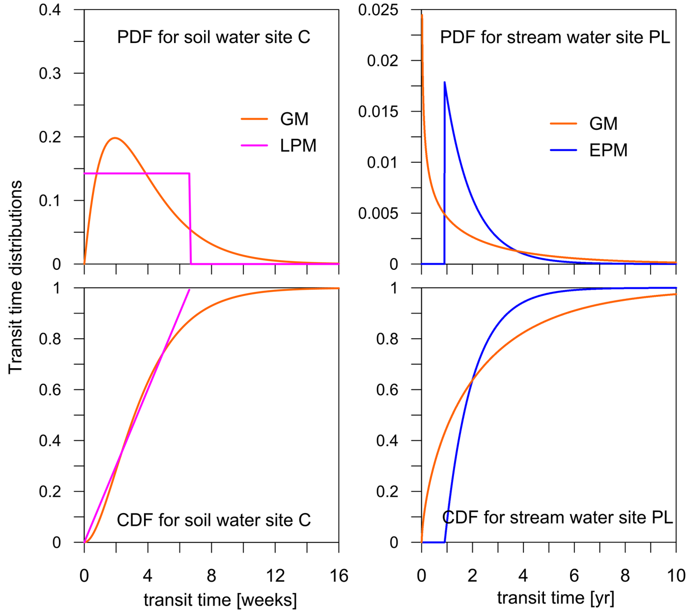

Figure 8. Distribution functions depicted as Probability and Cumulative Density Functions (PDF and CDF) of two characteristic sampling sites: C soil water site to the left and PL stream water site to the right, using two lumped models for each case.

HESSD
11, 12443–12488, 2014